THE USE OF REMOTE SENSING IMAGERY FOR EVALUATION OF POST-WILDFIRE SUSCEPTIBILITY TO LANDSLIDE AND EROSION HAZARDS IN THE SALMON-CHALLIS NATIONAL FOREST, LEMHI COUNTY, IDAHO

Diane K. Sprague-Wheeler
Department of Geosciences
Idaho State University
Pocatello, ID 83209-8130

ABSTRACT

Remote sensing and field-based research is used to investigate landslide and soil erosion hazards resulting from wildfire activity in central Idaho. This study focuses on four areas in the Salmon-Challis National Forest (SCNF). Field-based research is performed on three sites (one kilometer (km^2) each) to test the remote sensing imagery and to use as ground-truth for the larger, fourth site (570 km^2). Two relative hazard maps, one for landslides and one for erosion, are developed for each of these areas. The classification system for the maps includes slope, aspect, burn severity, understory vegetation cover (for erosion only), hydrology, bedrock geology, and soil characteristics. Each parameter is assigned a relative hazard ranking of ordinal numbers. Results indicate that digital elevation models are useful in providing comprehensive slope and aspect analysis. High-resolution multispectral data can be used successfully to map areas of high burn severity and unburned areas, although mapping areas of low to moderate burn severities proved more difficult. The imagery can also be used to assess vegetation cover; however, it cannot distinguish between understory and overstory vegetation cover. The kappa statistic is used to assess the accuracy of the remote sensing data. Results indicate that the remote sensing data corresponds well to field mapping when using a bootstrap accuracy check. However, in the pixel-by-pixel comparison, kappa values are considered low. The greatest difference between the relative hazard maps using field data and remote sensing is that the imagery classifies each 4-meter pixel, whereas field mapping tends to classify larger areas based upon similar features. This study has produced a well-documented methodology of landslide and soil erosion hazard assessment and a qualification of the relative importance of land cover parameters in the SCNF.

Keywords: GIS, satellite

INTRODUCTION

PROBLEM STATEMENT

The 2000 wildfires of central Idaho burned thousands of square kilometers of forest and grazing land and are estimated to have cost millions of dollars in firefighting and damage to infrastructure, natural resources, and the environment (USFS, 2001a). It may be impossible to assess the full extent of damage to natural resources and the pristine environments of areas such as the Salmon-Challis National Forest (SCNF) (Figure 1). One detrimental effect of large wildfires is the widespread impact of increased landslides and soil erosion by water resulting from the removal of vegetation (Bailey, 1971; McKean et al., 1991; Dragovich et al., 1993a,b). Sediment transport in burned areas affects watersheds and water quality for aquatic wildlife. Degradation of wildlife habitat is accelerated by sediment loading of streams from landslides. Sediment and other materials transported after fires may be deposited in stream channels, which may change stream morphology, especially channel form, and particle size and distributions. In addition, wildfires affect new vegetation growth and this affects habitat, sediment stability, and future wildfire regimes.

Currently, field study is the primary tool for investigating the potential for landslides and erosion after wildfires (Benavides-Solorio and MacDonald, 2001; Cannon, 2001; Cannon et al., 2001a,b; Meyer et al., 2001). This can be especially difficult and time-consuming in remote areas with limited access and large, diverse landscapes. For example, the SCNF, located in central Idaho, contains over 10,000 square kilometers (km²) of land. This area is extensive and heavily forested; thus field investigations to identify and map landslide and soil erosion hazards are limited. This study evaluates the

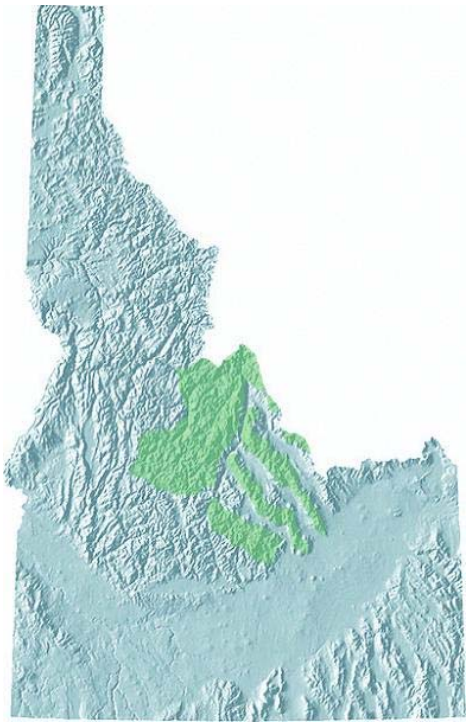

Figure 1. Topographic map of Idaho. Areas highlighted in green indicate the approximate location of the Salmon-Challis National Forest.

usefulness of remote sensing imagery in assessing relative landslide and erosion hazards and develops a relative hazard ranking system for landslide and erosion hazards in the SCNF. This methodology was first developed and validated on three one-km² sites, and then applied to a 570 km² area of the SCNF to assess large-scale applicability. The hypothesis of this study is that field studies and remote sensing methods can be used to identify land cover parameters that influence susceptibility to post-fire erosion and landslides.

BACKGROUND

Wildfire History

Decades of fire suppression have led to an unnatural buildup of fuels within forests, contributing to the development of intense wildfires (USFS, 2001b). Complete fire suppression has disrupted normal ecological cycles and changed the structure and make-up of forests. Years of fire suppression have created fuel ladders, and consequently forests experience more of the high-severity, stand-replacing fires. In addition, a general warming cycle over the past century is thought to have increased the frequency of wildfires (Meyer et al., 1992). As noted by the United States Forest Service (USFS) (2001b), decades of aggressive fire suppression have drastically changed the look and fire behavior of forests and rangelands. Compared to forests a century ago, forests today are denser and have smaller, less fire-resistant trees. The composition of forests has changed from more fire-resistant species such as ponderosa pine, aspen, and cottonwood, to non-fire resistant species such as grand fir, Douglas fir, and lodgepole pine (Gough and Lamb, 2000; Idaho Forest Products Commission, 2003; Keep Idaho Green, 2003). As a result, studies show that wildfires today tend to burn hotter and faster than those of the past (USFS, 2001b).

Scientists have understood for some time that fire is an essential part of the forest ecosystem. Not only are forests adapted to wildfires, they are in large part dependent upon them. For example, lodgepole pine produces two types of cones. As noted by Carey and Carey (1989), one type opens upon reaching maturity and falls to the ground, where, unless it lands in a nurturing (i.e., soil and nutrient rich) environment, it is quickly eaten by rodents and birds. The other type of cone only opens at temperatures of 49º Celsius (C), an unlikely temperature to be reached in forests without fire. Fires leave behind a rich ash bed in which the seeds from these cones can quickly germinate and become established. Plants normally rely on the slow decomposition of organic material for their nutrients, and ash from fire contains a dense concentration of these nutrients. Ash provides a natural fertilizer for plants and does not require additional breakdown to be accessible to the root systems of the plants. Higher levels of sunlight resulting from the destruction of forest canopy also stimulate plant growth. Carey and Carey (1989) report that when old-growth timber is removed, total plant species increase thirty-fold within 3-20 years. Streams benefit from fire to some extent by the addition of ash that increases in-stream vegetation, and by increased available sunlight that increases water temperature and stimulates aquatic productivity.

There are numerous wildfires every year in the U.S. Between the 40-year period of 1960-2000, there was an average of 135,826 wildfires and 16,415 km² burned each year (NIFC, 2001) (Table 1). The largest number of fires occurred in 1981, while the most area burned in 2000. Wildfires are started in a variety of ways, including lightning

Table 1. Total wildfires and area burned in the U.S. between the 40-year period of 1960-2000 (NIFC, 2001).

Year	Number of Fires	Area Burned (km^2)	Year	Number of Fires	Area Burned (km^2)
2000	122,827	34,084	1979	163,196	12,087
1999	93,702	22,913	1978	218,842	15,827
1998	81,043	9,428	1977	173,998	12,758
1997	89,517	14,863	1976	241,699	20,679
1996	115,025	27,120	1975	134,872	7,249
1995	130,019	9,371	1974	145,868	11,651
1994	114,049	19,117	1973	117,957	7,751
1993	97,031	9,350	1972	124,554	10,688
1992	103,830	9,946	1971	108,398	17,314
1991	116,953	9,056	1970	121,736	13,268
1990	122,763	22,067	1969	113,351	27,070
1989	121,714	13,200	1968	125,371	17,126
1988	154,573	29,942	1967	125,025	18,853
1987	143,877	16,805	1966	122,500	18,512
1986	139,980	13,388	1965	113,684	10,733
1985	133,840	17,947	1964	116,358	16,986
1984	118,636	9,171	1963	164,183	28,817
1983	161,649	20,560	1962	115,345	16,507
1982	174,755	9,640	1961	98,517	12,287
1981	249,370	19,482	1960	103,387	18,123
1980	234,892	21,290			

strikes and human activities, such as campfires, smoking, incendiary, equipment, railroads, juveniles, and miscellaneous (NIFC, 2001). During 1988 to 1997, lightning strikes were responsible for burning the most area while miscellaneous human activities caused the greatest number of fires (Table 2).

Lightning strikes were a major contributing factor to the extensive wildfires that occurred in the western U.S. during summer 2000. These wildfires were a result of two primary factors: drought-like conditions accompanied by dry storms that produced thousands of lightning strikes and windy conditions, and an unnatural buildup of brush and trees created by the effects of aggressively suppressing all wildfires for more than a century (USFS, 2001b). Two of the largest of these fires, the Clear Creek Fire and the Salmon-Challis Forest Wilderness Fire, occurred within the SCNF. Collectively these two fires are known as the Salmon-Challis National Forest Fire; they burned approximately 1,619 km^2 of forest and grazing land. This fire, one of the top five largest fires in the U.S. during 2000, is estimated to have cost millions of dollars in firefighting and damage to infrastructure, natural resources, and the environment (NIFC, 2001).

Table 2. Number of wildfires and area burned in the U.S. by cause between the 10-year period of 1988-1997 (NIFC, 2001)

Year	Cause	Number of Fires	Area Burned (km²)
1988	Human	138,238	14,403
	Lightning	16,335	15,539
1989	Human	107,318	8,419
	Lightning	14,396	4,791
1990	Human	105,784	7,023
	Lightning	16,979	15,052
1991	Human	104,777	7,091
	Lightning	12,164	1,961
1992	Human	89,701	5,699
	Lightning	14,245	4,244
1993	Human	87,725	4,720
	Lightning	9,305	4,626
1994	Human	94,265	7,751
	Lightning	19,801	11,379
1995	Human	120,045	5,886
	Lightning	9,974	3,489
1996	Human	99,606	13,618
	Lightning	15,560	13,504
1997	Human	79,484	3,985
	Lightning	10,033	10,836
10-Year Average	**Human**	**102,694**	**7,859**
	Lightning	**13,879**	**8,542**

Mass Wasting/Erosion Terminology

There are numerous types of surficial processes defined in the literature, so it is prudent to define the terminology used in this study. This study considers the propensity for rapid mass wasting, rather than distinguishing the specific mechanisms and types of mass wasting. Mass wasting is a general term that can include landslides, slumps, debris flows, mud flows, earth flows, rock falls, soil creep, etc.

This study focuses on landslides and flows, because these are the two processes most likely to affect water quality within watersheds. Landslides are defined as the rotational or planar movement of a discrete mass that takes place along a well-defined failure surface. A flow has continuous, internal deformation without the development of a failure surface. Many types of flows are recognized in the literature, and flows observed in motion are generally classified by the type and rate of movement, whereas flows not observed in motion are classified by the morphology and sediment type of flow deposits (Easterbrook, 1999). Herein, this study will use the term landslide to include all landslides and flows.

Flowing water removes soil from slopes through a variety of erosional processes, including sheet wash, rilling, and gullying. As noted by Selby (1993), sheet wash is the process by which soil is detached due to raindrop impact and entrained by water runoff. Flow velocities typically range

from 0.015 to 0.30 meters (m) per second. Rills are small channels, a few centimeters (cm) to tens-of-centimeters in cross-section, that are usually discontinuous and not connected to a stream channel system. Rills may deepen and widen to form gullies. Gullies are typically over 0.3 m wide and 0.6 m deep. Herein, this study will use the term erosion to include the processes of sheet wash, rilling, and gullying.

The Relationship Between Wildfires and Landslides/Erosion

Undisturbed lodgepole and ponderosa pine forests typically have high infiltration rates, lack overland flow, and experience low erosion rates (Benavides-Solorio and MacDonald, 2001). Reduction of infiltration rates can lead to overland flow (e.g. sheet wash) and increased rill erosion. Wildfires can make forests more susceptible to sediment transport processes in a number of ways. For example, fires may create water repellent soils, they may remove the protective layer of litter/duff covering the forest floor, and they may remove vegetation that stabilizes slopes and reduces surface runoff.

Numerous studies have observed a wettable surface layer that overlies a water-repellent layer following fires in watersheds. Water repellent soils are those which will hold a drop of water for at least a few seconds before penetration (Doerr et al., 2000). Strong water repellency can be created when vaporized organic compounds move downward due to the temperature gradient and condense in lower soil layers. Doerr et al. (2000) observed little change in water repellency of soils at temperatures less than 175º C. At temperatures between 175-200º C water repellency was intensified. Hydrophobic substances are fixed to soil particles around 250º C, but destroyed above 270-300º C. These findings indicate that cooler fires will cause water repellency at the surface, and hotter fires will produce water repellency at greater depth. Soil temperatures would be highest at the ground surface during a fire and decrease with depth. Repellency is increased with longer sustained heating times. The longevity of water repellency is hard to predict because it is very site specific and depends on soil temperature, soil type, organic compounds, and climatic conditions. Several studies indicate that water repellency can cause reduction in soil infiltration capacity, enhanced overland flow and accelerated erosion, development of preferential flow, rainsplash detachment, soil loss by both water and wind, and generation of debris flows (Doerr et al., 2000; Benavides-Solorio and MacDonald, 2001; Huffman et al., 2001; Meyer et al., 2001).

Wildfires may burn away the protective litter layer on the forest floor and thus increase the rate of precipitation delivery to the soil and the occurrence of rainsplash detachment (Martin and Moody, 2001). This results in higher rates of surface runoff and erosion. Most studies indicate that the greatest increase in runoff and erosion occur within the first few years after the wildfire, but this is dependent upon climatic conditions.

Fires may also destroy vegetation that removes moisture from the soil via evapotranspiration, which may eventually lead to increased overland flow. In addition, vegetation increases slope stability and thus the removal of small types of vegetation, such as bushes and grass, has immediate consequences for erosion. Similar to the removal of litter, this results in higher rates of surface runoff and rainsplash detachment, and increases the rate at which precipitation is delivered to the soil (Cooke and Doornkamp, 1990). Large tree roots are effective in making slopes less susceptible to deep-seated landslides (Selby, 1993). Tree roots near the surface can

be completely incinerated by high-severity fires. In some cases, the roots can be burned but it will take 5-6 years for them to completely decay, at which time they are rendered useless for slope stability (Meyer et al., 2001). It has been suggested by various studies that shallow landslides are more probable in burned and/or logged areas after the tree roots decay, an effect that occurs 4-10 years after tree mortality (Gray and Megahan, 1981; Clayton and Megahan, 1986; Meyer et al., 2001).

Setting

The study area is the Yellowjacket Mountains in the SCNF, Lemhi County, Idaho (Figure 2). Much of the study area is very steep, with narrow canyons and slopes up to 40º (Figure 3). The elevation generally ranges from 2,000-3,000 m (all elevations are above sea level).

Four specific study sites were selected for this study (Figures 2, 3). Sites #1 and #2 are located within the Panther Creek watershed. Panther Creek, a tributary to the Middle Fork of the Salmon River, drains a 1,378 km² area within the Middle Salmon-Panther subbasin. Site #3 is located within the Camas Creek watershed, which is part of the Lower Middle Fork of the Salmon River subbasin. Camas Creek is also a tributary to the Middle Fork of the Salmon River. These particular sites were selected due to their varying slopes and aspects, burn severity, amount of understory vegetation cover, hydrology, bedrock geology, and soil characteristics in order to provide a diverse range of conditions for this study. Site #4 is a 570 km² area of the SCNF that was selected to encompass the three smaller study sites.

As noted by B. Rieffenberger (oral comm., 2002), these subbasins have a wide range of climates due to varying elevations, and local topography and aspects. Climate can range from a near desert environment in lower elevations to near alpine environment in upper elevations. Maximum summer temperatures can exceed 38° C in the lower elevations, and winter temperatures can be well below -18° C at all elevations. Snowfall contributes most of the annual precipitation, although rain is common in late spring and early summer. High-intensity, short-duration thunderstorms occur primarily in July and August. These storms tend to move in an easterly direction along the Salmon River Canyon. In the study areas, located south of the Salmon River Canyon, thunderstorms generally approach from the west or from the north. The average precipitation ranges from 38 cm per year along the lower elevations to 102 cm per year at the higher elevations.

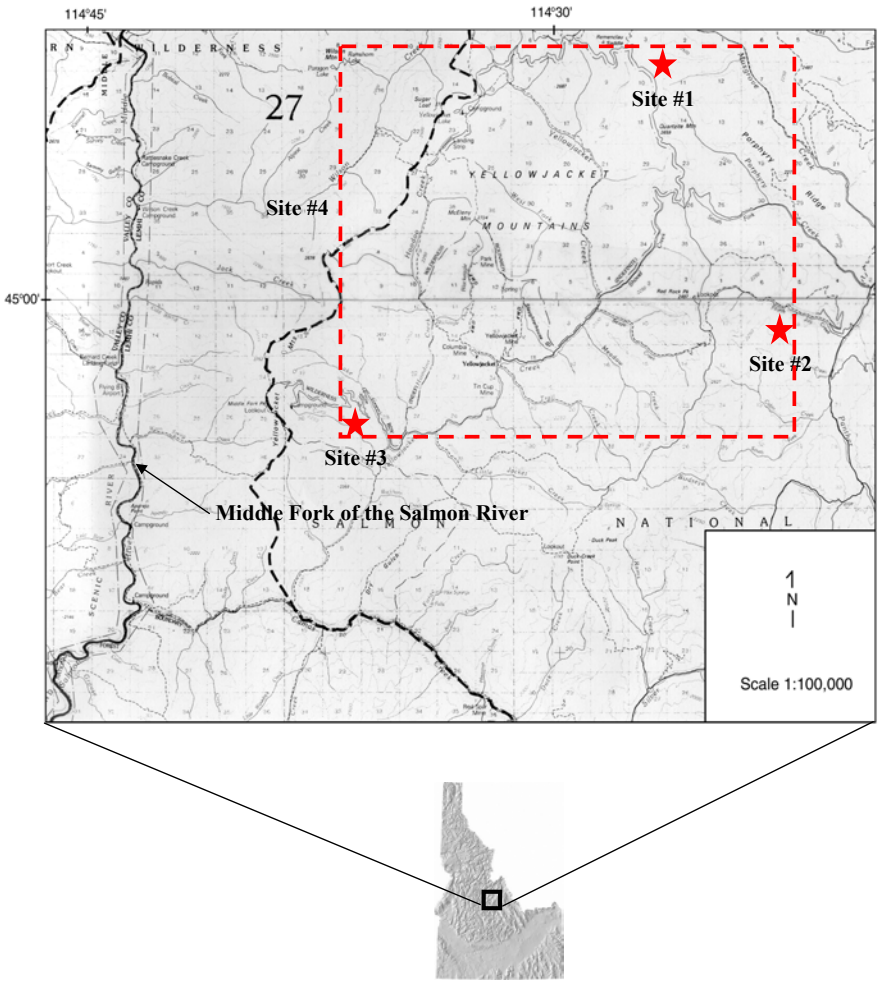

Figure 2. Map showing the approximate locations of the four selected study areas within the Yellowjacket Mountains in the Salmon-Challis National Forest, Lemhi County, Idaho (modified from Idaho Transportation Department, 1996). Sites #1-3 are indicated in red.

Figure 3. Relief map of Site #4 and the approximate locations of Sites #1-3 (indicated by red stars). Streams are shown by blue lines. (Derived from IKONOS imagery, 4-m resolution.).

Landforms within the watersheds of the Middle Fork of the Salmon River are highly variable. The lower elevations tend to consist of oversteepened canyons and rock outcrops. The middle elevations are characterized by mountainous slopes ranging from 10° up to 40°. Upper elevations are dominated by broad and gently-sloping ridge tops and mountain slopes.

The watersheds of the Middle Fork of the Salmon River are dominantly subalpine and Douglas fir forests, and include ponderosa pine, lodgepole pine, and Douglas fir (Rieffenberger, 2000). Lodgepole pines are common especially in old burn areas. The forest undergrowth consists primarily of bunchgrass, pinegrass, and beargrass.

PREVIOUS WORK

Geologic Mapping

Ross (1934) first mapped the geology of the Yellowjacket Mountains. It has been geologically mapped and interpreted most recently by Ekren (1988), Evans and Connor (1993), Winston et al. (1999), and Tysdal (2000). A compilation of these maps has been constructed for this study (Figure 4). There are seven main bedrock types significant to the study areas. They include (1) the "Type" Yellowjacket Formation; (2) the Hoodoo Quartzite; (3) the informal argillaceous member of the "Cobalt" Yellowjacket Formation of the Middle Proterozoic Belt Supergroup (Winston et al., 1999); (4) Ordovician or Middle Proterozoic granites; (5) granitic rocks of the Idaho Batholith; (6) Tertiary granites of the Casto and Crags Plutons, and (7) the Challis Volcanic Group. Each of these seven main bedrock types possesses distinct soil-forming and sediment yield characteristics.

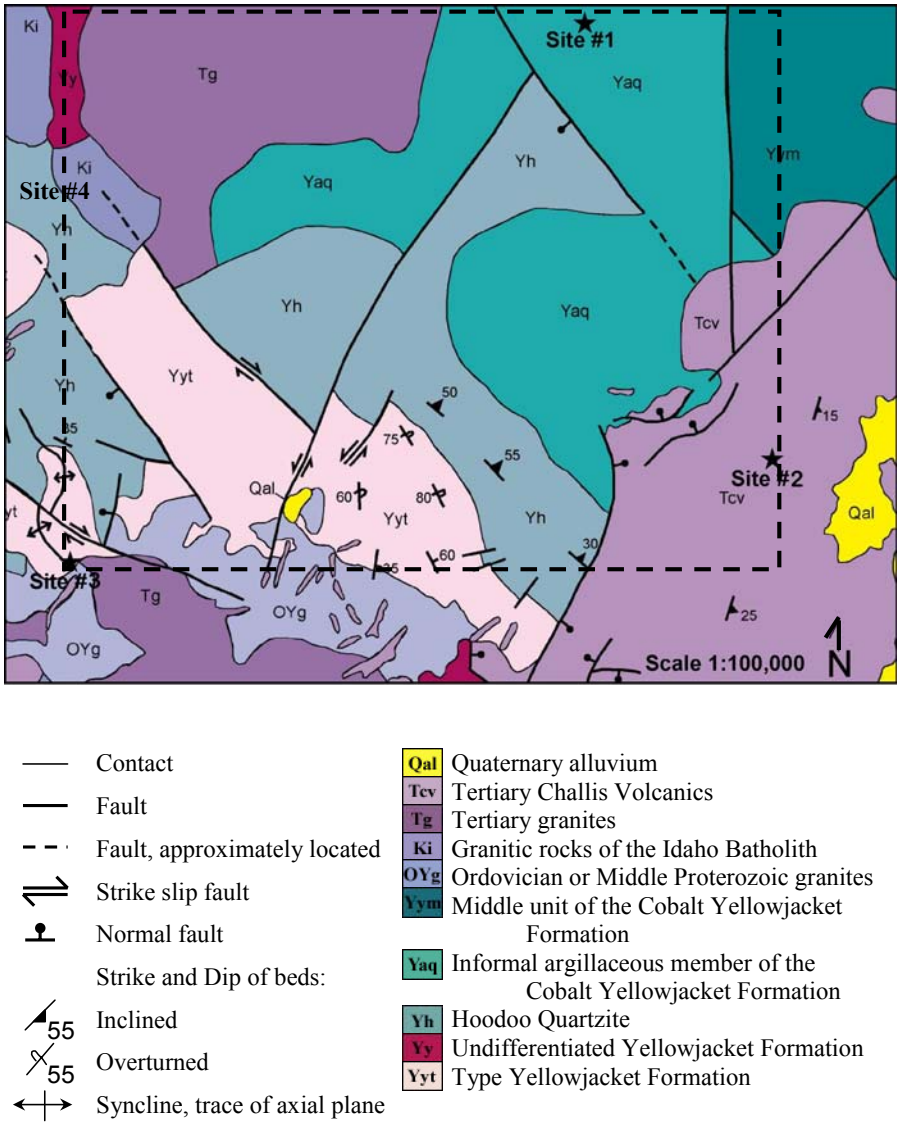

Figure 4. Simplified geologic map of the study areas compiled from Ross (1934), Ekren (1988), Evans and Connor (1993), and Winston et al. (1999). Sites #1-3 are indicated by black stars and Site #4 is bound by the thick black dotted line.

Type Yellowjacket Formation

Since its first usage by Ross (1934), the name Yellowjacket Formation has been generously applied to any slightly metamorphosed, nonfossiliferous, medium to dark gray, micaceous quartzite and siltite of Middle Proterozoic age in central Idaho. The name Yellowjacket Formation as used in this inclusive sense is stratigraphically located both above and below the Hoodoo Quartzite. Winston et al. (1999) determined that the Type Yellowjacket is in conformable contact below the Hoodoo, and thus they subdivided the unit formerly lumped together as "Yellowjacket" into the Type Yellowjacket, which lies below the Hoodoo, and the Cobalt Yellowjacket, which lies above the Hoodoo.

The Type Yellowjacket Formation is correlative to the informal lower member of the Yellowjacket as described by Evans (1999). It is primarily composed of gray to greenish-gray siltite and argillaceous siltite with minor carbonate and fine-grained quartzite layers. It is primarily slope-forming and weathers to sand and silt; thus movement may occur as debris flow or as soil creep in those areas with relatively thick soil development.

Hoodoo Quartzite
The Hoodoo Quartzite is generally massive, although intricately jointed in some places (Ross, 1934; Ekren, 1988). Bedding is indistinct; however, beds 0.3-1.0 m thick can be found that are distinctly crossbedded (Ekren, 1988). This unit is indurated and fairly resistant to weathering. Little or no movement is expected to occur in this unit, as this rock weathers into angular fragments of quartzite.

Argillaceous Quartzite of the Cobalt Yellowjacket Formation
The Cobalt Yellowjacket Formation is correlative to the informal middle and upper members of the Yellowjacket as described by Evans (1999). Winston et al. (1999) further subdivides the middle member, the lower section that stratigraphically overlies the Hoodoo Formation, as the informal argillaceous quartzite member of the Cobalt Yellowjacket Formation. This lower section is composed of light gray siltite and fine-grained quartzite alternating with black argillite. Sand and silt consistently penetrate downward into cracks developed within the argillite layers. Large (30 cm-scale) trough and planar cross-beds and hummocky cross stratification are common. Also present are ripple cross-laminations and local rip-up clasts (Tysdal, 2000). This member is primarily slope-forming and weathers to sand and silt. Movement may occur as debris flow or as soil creep in those areas with relatively thick soil development.

Ordovician or Middle Proterozoic Granites
The Ordovician or Middle Proterozoic granites are intrusive rocks that consist of diorite, quartz diorite, gabbro, granite, syenite, and quartz syenite (Ross, 1934; Ekren, 1988). These rocks are primarily ledge-forming and weather to form grus.

Granitic Rocks of the Idaho Batholith
The Mesozoic granitic rocks of the Idaho batholith include undifferentiated granitic rocks, migmatite, quartz diorite, and quartz monzonite (Ross, 1934). These rocks are primarily ledge-forming and weather to form grus.

Tertiary Granite
The Tertiary granites include the Eocene granitic rocks of the Casto Pluton and the Crags Pluton (Ross, 1934; Ekren, 1988). The Casto Pluton consists of pink granite and light-gray quartz monzonite. The granites of the Crags Pluton include quartz monzonite and granodiorite. These granites are ledge-forming and weather to form grus.

Challis Volcanic Group
The Eocene Challis Volcanic Group unconformably overlies all Proterozoic units. As noted by Fisher and Johnson (1995), the Challis Volcanics range from magnesium-rich basalt to alkali rhyolite. The predominant rock is intermediate in composition (dacite and rhyodacite). The Challis Volcanics include voluminous ash-flow tuffs, lavas, and hypabyssal intrusives

interbedded with fluvial and lacustrine sedimentary rocks. Hydrothermally altered rocks, which are typically highly silicified, bleached, and stained with iron oxides, are common. The Challis Volcanics are intruded by the pink granites of the Casto Pluton. The Challis Volcanics are ledge-forming and weather to medium- to fine-grained sand. Movement may occur as debris flow or as soil creep in those areas with relatively thick soil.

Remote Sensing Studies

Several studies have investigated the applicability of remote sensing methods to assess landslide hazards. Moeremans and Dautrebande (2000) used synthetic aperture radar (SAR) imagery to evaluate spatial and temporal soil moisture variation, which is crucial information for hydrologists wanting to predict flood events. Kimura and Yamaguchi (2000) demonstrated that SAR data can be used to investigate kilometer-scale landslides by using interferograms to detect and evaluate displacement patterns and landslide behavior. McKean et al. (1991) used Landsat Thematic Mapper (TM) imagery to explore the effect of vegetation type on debris flow occurrence. They found root strength and evapotranspiration to be important variables in the occurrence of shallow landslides. McKean et al. (1991) found that remote sensing can be used to measure soil depth indirectly by the type of vegetation present. Pickup and Marks (2000) used airborne gamma radiometrics and digital elevation models (DEMs) to investigate patterns of erosion and deposition by analyzing K, Th, and U content. Gamma ray signatures of these elements are determined by lithology but change with weathering, erosion, and deposition. Nachtergaele and Poesen (1999) assessed ephemeral gully erosion rates by utilizing temporally sequential high-altitude stereo aerial photographs. Singhroy et al. (2000) and Singhroy and Mattar (2000) evaluated the usefulness of interferometric SAR (InSAR) and high-resolution (8 m) RADARSAT imagery in identifying meter-scale landslide features, thereby assisting in hazard mapping. They found InSAR data to be the most useful for detailed geomorphic characterization and identification of landslide features in high relief terrains, and RADARSAT data useful for identifying more regional landslide features in mountainous areas.

Landslide Studies

Many studies have investigated landslide hazards. A review of several studies particularly relevant to this study is provided in this section.

Meyer et al. (2001) conducted sediment transport studies in the South Fork Payette River basin in west-central Idaho. They found evidence to indicate that sediment yields in this region are not constant over time, and that climatic variations and related fire regime changes may exert a strong influence on the probability of major erosional events. This study compared sediment yields in the study area to longer term estimates of sediment yields by alluvial fan stratigraphy and work by other investigators. This study also investigated the distinction between saturation-failure events and runoff-generated events after fires and their differing causal factors. Meyer et al. (2001) found that after stand-replacing fires in the Idaho batholith region, storms of sufficient intensity and duration can initiate sediment transport in the form of large debris flows to flood events. Sediment-charged flows are initiated by different mechanisms and at different times over the post-fire period. Intense precipitation occurring within the first few post-fire years produces runoff from bare, burned slopes, which creates progressive sediment bulking on slopes and in channels. Runoff-related events are suppressed by vegetation regrowth, the litter layer, and the lessening of water-repellent soil conditions within the first 5 years or so following fire. Several

years after fire when tree root strength has been lost, saturation and failure of colluvium occurs during prolonged and heavy winter-spring rainfall and often with snowmelt. Slopes remain susceptible to saturation-induced slope failures until deep roots have been reestablished, regardless of vegetation regrowth.

Cannon (2001) and Cannon et al. (2001a,b) have extensively studied debris flow initiation after fires in drainage basins located in Colorado, New Mexico, and southern California. Their studies indicate that debris flows are not the dominant erosive response from burned basins; rather, most of the burned basins evaluated produced sediment-laden streamflow or no discernible response. They classed debris flows into two groups, Type 1 and Type 2. Type 1 debris flows consist of poorly sorted, matrix supported, and up to boulder-sized materials. Most of these types of flows are initiated through a process of progressive sediment bulking of surface runoff. These flows are produced from basins in which 5-100% of the basin experienced moderate to high burn severity. Most of these flows occur without the presence of a water-repellent soil layer. Type 2 debris flows consist primarily of poorly-sorted sand and gravel-sized material in an abundant matrix that is rich in charcoal and ash. Type 2 debris flows transport finer material and thus are less destructive than Type 1 debris flows. Type 2 debris flows appear to be initiated exclusively through runoff dominated processes, and tend to occur in areas with a discontinuous water-repellent layer. They may be produced from basins that experience anywhere from 8-100% burn.

Gritzner et al. (2000) utilized 30-m DEM's to test Geographic Information System (GIS) modeling, chi-square analysis, Bayesian probability modeling, and cumulative frequency curves to predict landslide locations in the Middle Fork Payette River basin in Idaho. Evidence suggests that slope and elevation are significantly related to landslide occurrence in the study area. They attribute the perplexing relationship between elevation and landslides to the location of logging roads at certain elevations. The locations of these logging roads were not adequately mapped so they could not be included in the input data. Their study found that GIS offers a useful method of documenting many key variables driving landslide risk and developing maps of landslide hazard, and that usefulness of this methodology is limited by the coarse resolution of the 30-m DEM's.

Benavides-Solorio and MacDonald (2001) used field study and rainfall simulation on small plots of land in the Colorado Front Range to evaluate those factors contributing to landslide hazards in Colorado. Site variables such as burn severity, percent vegetative cover, soil water repellency, soil moisture, time elapsed since burning, and slope angles were evaluated in relation to how they corresponded to runoff and sediment yields. Final analysis indicated that burn severity did not significantly affect runoff rates, but had a significant impact on the sediment yield. Sediment yield of high-severity fire plots produced 4.5-4.8 times as much sediment as moderate severity plots, and 10-26 times as much sediment as low severity and unburned plots. A similar study by Johansen et al. (2001) indicates that the runoff from burned plots was about 45% of the total precipitation applied, and only 23% from the unburned plots. However, burned plots generated 25 times more sediment than unburned plots.

METHODS

FIELD STUDY

The three specific study areas (Sites #1-3) within the Yellowjacket Mountains were identified during June of 2001 (Figures 2, 3). Site #4 was evaluated with remote sensing data only and is discussed in Chapter 3. Sites #1-3 are approximately one km² each and were selected due to the varying slopes, aspects, burn severity, amount of understory vegetation cover, hydrology, bedrock geology, and soil characteristics exhibited. These parameters were mapped in the field during June, July, and August of 2001 and 2002.

In order to assess the relative landslide and erosion hazards of the study areas, two relative hazard classification systems were developed for this study. One relative hazard classification system is specifically for landslides, and considers parameters including: slope, aspect, burn severity, hydrology, bedrock geology, and soil characteristics (Table 3). The other relative hazard classification system is specifically for erosion, and considers the same parameters with the addition of understory vegetation cover (Table 4). In order to develop a relative hazard map, every parameter within each system was assigned a relative hazard ranking of ordinal numbers 0-10, with 10 being more likely to influence the occurrence of landslides or erosion and zero most likely to have no effect. This range was specifically selected so that parameters could be given different weighting in the classification system. For example, parameters hypothesized to have more influence on the occurrence of landslides and erosion were assigned values closer to 10, whereas parameters hypothesized to have less influence on the occurrence of landslides and erosion were assigned values closer to zero. The rankings of each parameter were compared to other parameter ranking values within the classification system in order to verify that the numbers were accurately weighted. For example, it is hypothesized for this study that an area of high burn severity (ranked with a value of 10) has the same propensity for landslides and erosion as an area with surface water present (also ranked with a value of 10). The following sections describe the assignment of ordinal numbers to the aforementioned parameters.

Table 3. Relative hazard ranking values for landslides within study areas (SF = Safety Factor).

Slope	Aspect	Hydrology
>55° (SF < 0.5) = 10 35-55° (0.5 ≤ SF < 1.0) = 9 20-34° (1.0 ≤ SF ≤ 2.0) = 2 0-19° (SF > 2.0) = 1	North = 1 East & West = 2 South = 3	Surface water present = 10 Surface water not present = 0
		Geology
		Sandstones/siltstones = 1 Granites = 2 Challis Volcanics = 4
	Burn Severity	**Soil Characteristics**
	High = 10 Moderate = 9 Low = 8 Unburned = 0	Sand = 4 Silt = 5 Clay = 3

Table 4. Relative hazard ranking values for erosion within study areas.

Slope	Aspect	Hydrology
50-90° = 10 45-49° = 9 40-44° = 8 35-39° = 7 30-34° = 6 25-29° = 5 20-24° = 4 15-19° = 3 10-14° = 2 5-9° = 1 0-4° = 0	North = 3 East & West = 2 South = 1	Surface water present = 10 Surface water not present = 0
	Burn Severity	**Geology**
	High = 10 Moderate = 9 Low = 8 Unburned = 0	Sandstones/siltstones = 1 Granites = 2 Challis Volcanics = 4
	Understory Vegetation Cover	**Soil Characteristics**
	0-25% = 5 26-50% = 4 51-75% = 3 >75% = 2	Sand = 4 Silt = 5 Clay = 3

Slope

Slope is perhaps one of the most significant factors influencing landslides and erosion (Dunne and Leopold, 1978; Ritter et al., 1995; Wilson et al., 2001). Slope was measured quantitatively in the field using a hand-held clinometer. Slope rankings are calculated differently for landslides and erosion, because the factors that influence these processes are different. For landslides, slope stability represents a balance between driving forces (shear stress) and resisting forces (shear strength). This ratio is known as the Factor of Safety equation (Ritter et al., 1995):

$$\text{Factor of Safety} = \frac{c + (\gamma h \cos^2\theta - ')\tan\phi}{(\gamma h \sin\theta \cos\theta)}$$

where c = cohesion, kilonewtons/square meters (kN/m²)
γ = weight, kilonewtons/cubic meters (kN/m³)
h = height of the water table above the slide plane, m
' = pore pressure, kN/m²
ϕ = friction angle, degrees
θ = slope angle, degrees

Shear stress and shear strength were not measured quantitatively in the field; therefore, slope rankings for the landslide hazard classification system were determined by calculating the Factor of Safety for slopes in the study areas between 0-90º (Figure 5, Table 5). Soils in the field areas are generally dry, and saturation values are assumed to be zero for this study. Soils are predominantly cohesionless and cohesion is expected to play a smaller role than the friction angle, thus cohesion values are assumed to be zero for this study. A friction angle of 35º was assumed to be representative of the soil types (mostly sandy) in the field areas.

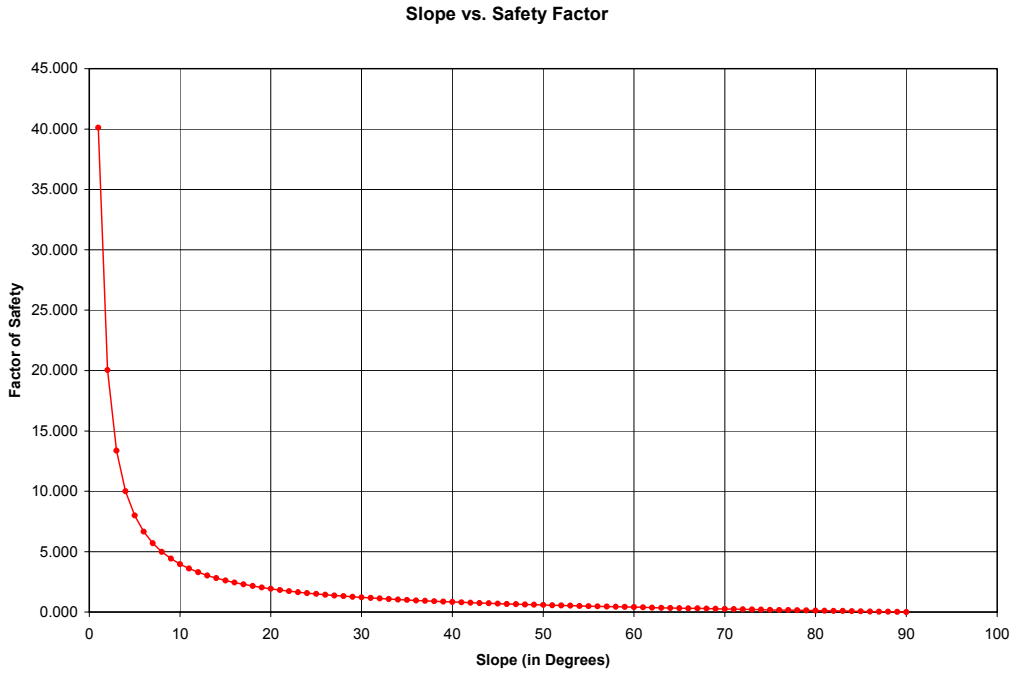

Figure 5. The relationship between slopes and Safety Factors (SF) in dry, cohesionless soils with a friction angle of 35º. Slopes with a SF greater than 1 indicate stable slopes, and values below 1 indicate a slope is prone to failure.

Slopes with a Safety Factor greater than 1 indicate stable slopes, and values below 1 indicate slope failure. Therefore, slopes with a Safety Factor greater than 2 (0-19º) are assumed to be most stable and ranked with a value of 1. Slopes with a Safety Factor of 1-2 (20-34º) are assumed to be stable and assigned a value of 2. Slopes with a Safety Factor of 0.5-1.0 (35-55º) have attained the critical value of 35º and are much more prone to failure than slopes of 34º or less; therefore, these slopes are ranked with a value of 9. Slopes with a Safety Factor less than 0.5 (greater than 55º) are assumed to be most prone to failure and assigned a value of 10.

Slope rankings for the erosion hazard classification system were determined by calculating the sine of the slope angle between 0-90º. In general, steeper slopes will be more prone to erosion due to several factors. The most important factor is the increasing shear stress with increasing slope steepness. In addition, water runoff will have a higher velocity on steeper slopes and thus be able to move more sediment and sediments with larger particle size. Rainsplash detachment on steeper slopes will move sediments greater distances down slope. For this study, it is hypothesized that erosion will increase with increasing slope (and hence, increasing shear stress). Therefore, slopes between 0-4º are ranked with a value of zero, slopes between 5-9º are ranked with a value of 1, and slopes between 10-14º are ranked with a value of 2. Slopes between 15-19º are ranked with a value of 3, slopes between 20-24º are ranked with a value of 4, and slopes between 25-29º are ranked with a value of 5. Slopes between 30-34º are ranked with a value of 6, slopes between 35-39º are ranked with a value of 7, slopes between 40-44º are ranked with a value of 8, and slopes between 45-49º are ranked with a value of 9. Slopes of 50º and greater are ranked with a value of 10, because such steep slopes will be highly prone to erosion where there is soil present.

Table 5. The relationship between slopes and Safety Factors (SF) in dry, cohesionless soils with a friction angle of 35º.

Slope, degrees	Safety Factor	Slope, degrees	Safety Factor	Slope, degrees	Safety Factor
1	40.115	31	1.165	61	0.388
2	20.051	32	1.121	62	0.372
3	13.361	33	1.078	63	0.357
4	10.013	34	1.038	64	0.342
5	8.003	35	1.000	65	0.327
6	6.662	36	0.964	66	0.312
7	5.703	37	0.929	67	0.297
8	4.982	38	0.896	68	0.283
9	4.421	39	0.865	69	0.269
10	3.971	40	0.834	70	0.255
11	3.602	41	0.805	71	0.241
12	3.294	42	0.778	72	0.228
13	3.033	43	0.751	73	0.214
14	2.808	44	0.725	74	0.201
15	2.613	45	0.700	75	0.188
16	2.442	46	0.676	76	0.175
17	2.290	47	0.653	77	0.162
18	2.155	48	0.630	78	0.149
19	2.034	49	0.609	79	0.136
20	1.924	50	0.588	80	0.123
21	1.824	51	0.567	81	0.111
22	1.733	52	0.547	82	0.098
23	1.650	53	0.528	83	0.086
24	1.573	54	0.509	84	0.074
25	1.502	55	0.490	85	0.061
26	1.436	56	0.472	86	0.049
27	1.374	57	0.455	87	0.037
28	1.317	58	0.438	88	0.024
29	1.263	59	0.421	89	0.012
30	1.213	60	0.404	90	0.000

Aspect

Slope aspect has been found to influence hillslope processes such as landslides and erosion in several studies (Crozier et al., 1980; Churchill, 1982; Dragovich et al., 1993a). Many studies have found that the greatest percentage of landslides occurs on equator-facing slopes, and only a small percentage occurs on pole-facing slopes. Selby (1993) notes that more insolated slopes in humid environments undergo more wetting/drying cycles with greater soil cracking. This leads to more macropore development, higher infiltration, and higher pore-water pressures. Increased soil cracking may also increase the water holding capacity, so that soils on sunny slopes may exceed or hold their liquid limit volume of water (Selby, 1993). However, Churchill (1982) found that erosion is more pronounced on pole-facing slopes in humid environments because the dry conditions on equator-facing slopes reduce weathering and fluvial erosion.

Slope aspect was evaluated in the field by using a Brunton compass. Since several studies have demonstrated that most landslides occur on equator-facing slopes, in the relative hazard classification system for landslides, southern slopes were assigned a value of 3, eastern and western slopes a value of 2, and northern slopes a value of 1. Due to Churchill's (1982) findings that erosion is more pronounced on pole-facing slopes, in the relative hazard classification system for erosion, southern slopes were assigned a value of 1, eastern and western slopes a value of 2, and northern slopes a value of 3. The parameter of aspect is hypothesized to have less influence on slope stability than the parameter of slope, hence the lower ranking values.

Burn Severity

Many studies have shown dramatic increases in the amount of landslides and erosion following forest fires (Benavides-Solorio and MacDonald, 2001; Cannon, 2001; Cannon et al., 2001a,b; Meyer et al, 1992; Meyer et al., 2001). This study considers burn severity to be a major factor influencing landslides and erosion, similar to the influence of slope. As defined by Key and Benson (2002), burn severity is the degree of environmental change caused by fire. Thus, field estimation of burn severity requires consistent judgment on the part of the observers.

For this study, two researchers evaluated burn severity in the study areas and compared findings to obtain as much consistency as possible. Burn severity was assessed by using the Landscape Assessment methodology (Key and Benson, 2002), which provides burn severity factor ratings as follows: % green is the percentage of crown foliage (living or dead) unaltered by fire relative to estimated pre-fire crown volume; % black is the black (non-living) crown foliage that actually caught fire, stems and leaves included, relative to estimated pre-fire crown volume; and % brown is the percentage of tree canopy affected by scorch or girdling, without direct flame contact, relative to estimated pre-fire crown volume plot-wide. In this study, areas with greater than 50% black are considered to be high severity and ranked with a value of 10. Areas with less than 50% black but greater than 50% brown are considered moderate severity and ranked with a value of 9. Areas with greater than 50% green and less than 50% brown or black are considered as low severity and assigned a value of 8. Unburned areas are not immune from landslides or erosion due to other factors (e.g., slope, surface hydrology), but the parameter of burn severity is intended to isolate burn effects. Therefore, unburned areas were assigned a value of zero.

Understory Vegetation Cover

Vegetation helps to stabilize slopes by various mechanisms and to varying degrees. Vegetation removes moisture from the soil via evapotranspiration, and roots enhance soil cohesion (Dragovich et al., 1993b). Leafy vegetation decreases the rate at which precipitation is delivered to the soil, so the absence of this type of vegetation may lead to erosion by surface runoff and rainsplash detachment. The presence of vegetation to intercept precipitation is particularly significant after storm events. Understory vegetation cover, such as brush and grass, is effective in reducing surface erosion such as rilling, gullying, and sheet wash, but is not significant in reducing large-scale mass movements such as landslides. Therefore, the ranking of understory vegetation cover is only relevant to erosion.

Understory vegetation cover was visually estimated in the field. For erosion considerations, slopes exhibiting understory vegetation cover from 0-25% are assumed to be less stable for the reasons previously stated, and were assigned a value of 5. Slopes with increasing cover are

assumed to be increasingly stable, and thus slopes with 26-50% cover were assigned a value of 4, slopes with 51-75% cover were assigned a value of 3, and slopes with greater than 75% cover were assigned a value of 2. The parameter of understory vegetation cover is hypothesized to have a slightly greater influence than the parameter of aspect, and much less influence than the parameters of slope and burn severity.

Hydrology

Areas with surface water present are significantly more likely to experience landslides and erosion than dry areas. This is because water is a primary contributor to erosion, and perched groundwater causes increased pore water pressure in soils which contributes to the increased likelihood of landslides (Dunne and Leopold, 1978). It is difficult to assess the influence of streams without an understanding of the hillslope hydrology, and it is not clear if streams within the study areas are fed by groundwater systems or originate from snow melt at higher elevations. Therefore, areas with surface water such as springs and streams were ranked with a value of 10. Areas lacking evidence of surface water are not immune from landslides or erosion due to other factors (e.g., slope, burn severity), but the parameter of hydrology is intended to isolate hydrological effects. Therefore, areas lacking evidence of surface water were ranked with a value of zero. The parameter of hydrology is hypothesized to have as much influence on slope stability as the parameters of slope and burn severity, and a much greater influence than the parameters of aspect and understory vegetation cover.

Bedrock Geology

The geology of Sites #1-3 was mapped in the field at a scale of 1:24,000; however, assigning a relative hazard classification system to the bedrock geology was fairly difficult because the relationships between rock lithology and landslides and erosion within the study areas have not been previously studied. In addition to the lithology, landslides may also be influenced by structural features, such as bedding planes and jointing, within the unit. Soil can slide down-slope along bedding planes in areas where dip-slopes are parallel to bedding (Dragovich et al., 1993a). Bedrock units that contain no bedding planes or significant jointing may be stronger than units that display these structural features. Lithology is assumed to have less influence on landslides and erosion than several other parameters considered in this study, so the parameter of bedrock geology was given less weight in the overall ranking.

As previously stated, there are seven main bedrock types within the study sites, and each bedrock type possesses distinct soil-forming and sediment yield characteristics. The Type Yellowjacket Formation and the Cobalt Yellowjacket Formation are primarily slope-forming and weather to sand and silt; thus movement may occur as debris flow or as soil creep in those areas with relatively thick soil development. These units within the study areas are ranked with a relative value of 1 because they are highly cohesive and have little soil development. Slopes are more prone to landslides in cases where the bedding plane orientation is the same as the slope direction; thus these areas would be assigned a value of 2. This circumstance was not evidenced in Sites #1-3, and the geologic map of Site #4 is at too gross of a scale (1:100,000) relative to the slope dataset (10 m) for determination of this circumstance. The Hoodoo Quartzite is highly indurated and fairly resistant to weathering. Little or no movement is expected to occur in this unit, as this rock weathers into angular fragments of quartzite. Areas with these lithologies are also ranked with a relative value of 1. The Ordovician or Middle Proterozoic granites, Mesozoic granitic rocks of the Idaho batholith, and Tertiary granites are primarily ledge-forming and

weather to form grus. This type of lithology is not as cohesive as the Type Yellowjacket and Cobalt Yellowjacket formations so these units are ranked with a value of 2. The Challis Volcanics are ledge-forming and weather to medium- to fine-grained sand. Movement may occur as debris flow or as soil creep in those areas with relatively thick soil development. A small meter-scale landslide was observed in the Challis Volcanics in Site #2 during year 2001 field studies, and this lithology is considerably more friable than the other relevant lithologies. Therefore, areas with this lithology are ranked with a value of 4. The parameter of bedrock geology is hypothesized to have a similar influence on slope stability as that of aspect, a slightly lesser influence than the parameter of understory vegetation cover, and much less influence than the parameters of slope, burn severity, and hydrology.

Soil Characteristics

Soil characteristics can influence landslides and erosion in two primary ways. First, different soil types have different infiltration capacities. Coarse-textured soils such as sands have larger pores that allow them to drain more easily than the fine pore structures in clays (Dunne and Leopold, 1978). As noted by Dragovich et al. (1993b), cohesive fine-grained soils are generally more likely to undergo deep-seated failures, and non-cohesive coarse-grained soils tend to fail by shallow processes.

The second important consideration is how easily soil can be transported, which affects erosion processes. Silt, which is smaller in size than sand, can be easily picked up by water and transported. Clay is more cohesive in nature, and thus is not as easily entrained. Taking all of these variables into consideration, silt was assigned a value of 5, sand a value of 4, and clay a value of 3. The parameter of soil characteristics is hypothesized to have a similar influence on slope stability as that of understory vegetation cover, a slightly greater influence than the parameters of aspect and bedrock geology, and much less influence than the parameters of slope, burn severity, and hydrology.

Soils were evaluated in the field by digging soil pits to bedrock depth, and then classifying the soil texture and color according to the Unified Soil Classification System (USCS)(McCarthy, 2002). Soil moisture and organic content were visually evaluated and, in general, soils were found to be dry with little organic content.

REMOTE SENSING STUDY

Potential sites for this study were first identified by using Landsat-7 Enhanced Thematic Mapper (ETM+) imagery and aerial photographs taken one month after the fires of summer 2000. The potential sites were compared to archived Landsat-5 TM data to contrast the amount of vegetation present prior to these fires.

Two IKONOS 11-bit images were used to evaluate the four sites chosen for this study. IKONOS is a commercial (owned by Space Imaging, Inc.) high-resolution Earth imaging satellite that provides 4-m multispectral spatial resolution. The two images were acquired September 9, 2001, at 18:40 and 18:41 Greenwich Mean Time (GMT) with a sun elevation of 48° and an azimuth angle of 159°. The multispectral data includes the following wavelengths of the electromagnetic spectrum: blue = 444.7-516.0 nanometers (nm); green = 506.4-595.0 nm; red = 631.9-697.7 nm; and near-infrared (NIR) = 757.3-852.7 nm. ENVI 3.5 (RSI, 2002) was used to mosaic and

evaluate the IKONOS imagery. The digital number (DN) values were converted to radiance values prior to all classifications by:

(DN_i) / (Radiometric Calibration Coefficient)
where i = 1 to z; z = number of pixels in image

Note: Radiance values were calculating based on conversion values provided by Space Imaging (Table 6).

Table 6. Calibration coefficients for IKONOS imagery (Space Imaging, 2002) (mW = megawatts, sr = steradian).

Radiometric Calibration Coefficient	Blue	Green	Red	NIR
$DN/(mW/cm^2 \times sr)$	728	727	949	843

Supervised and unsupervised classifications and transformations were then performed using all bands to determine which site parameters (burn severity, amount of understory vegetation cover, hydrology, bedrock geology, and soil characteristics) could be analyzed with the imagery. Burn severity and vegetation cover can be assessed with supervised classifications and transformations using ENVI 3.5 (RSI, 2002). It was not necessary to use IKONOS imagery to assess slope and aspect, as these features can be readily evaluated using 10-m DEM's. The hydrology within Sites #1-3 was in the form of small springs and streams less than 2 m, and so could not be detected by IKONOS data. Bedrock geology could not be assessed using IKONOS data because there are relatively few rock outcrops within the study areas, and most are obscured by vegetative cover. To assess the geology of Sites #1-4 remotely, a geologic map was compiled from pre-existing data mapped at a scale of 1:100,000 and digitized for this study. Soil type and soil characteristics are difficult to evaluate without adequate ground exposure and hyperspectral imagery. The following sections describe the assessments of burn severity and vegetative cover using IKONOS imagery.

Burn Severity Assessment

Burn severity can be mapped based on the reflectivity of soils and vegetation in the four multispectral bands. Burn severity was assessed by performing supervised and unsupervised classifications, and these classifications were then used to evaluate relative susceptibility to landslides and erosion. In contrast to supervised classifications, unsupervised classifications require minimal input from the analyst. The two unsupervised algorithms experimented with in this study were the IsoData and K-Means classifications. In these classifications, the software performs numerical operations that search for natural groupings of the spectral properties of pixels. The computer selects the class means and covariance matrices to be used in the classification. Neither of these algorithms produced results similar to the field mapping results.

Supervised classifications for burn severity were performed by selecting regions of interest or training classes that correlate with a specific burn severity (Figure 6). For example, there were four classes of burn severity mapped in the field (high, moderate, low, and unburned). An additional training class was developed for areas of high reflectance (outcrops, roads, and bare

ground) as these features would be incorrectly classified using burn severity classifications only. Thus a total of five training classes in each study site were utilized.

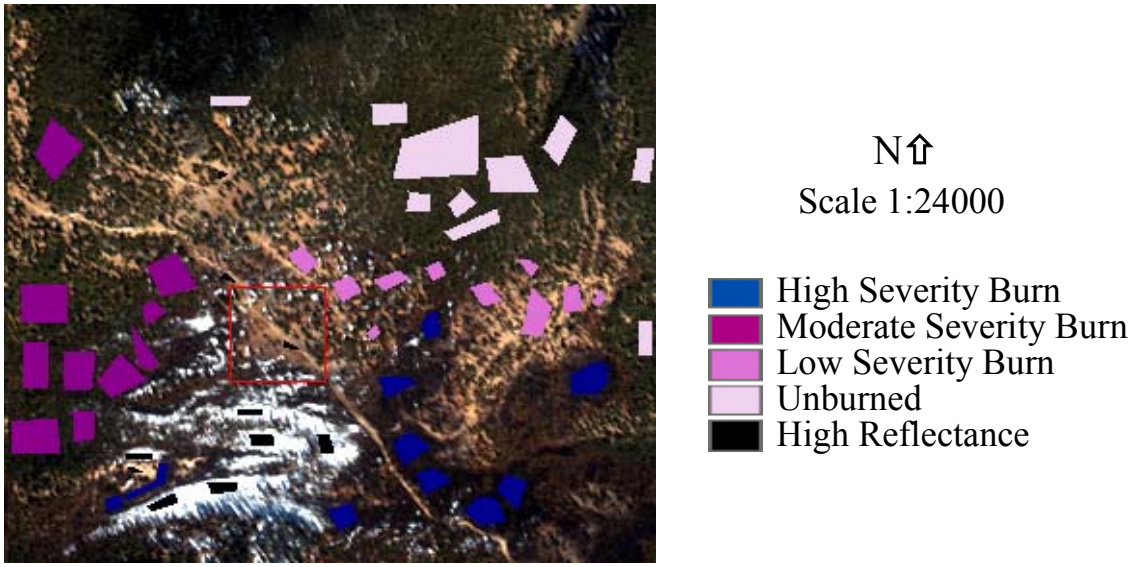

Figure 6. Training sites of Site #2. Red box indicates small meter-scale landslide observed during summer 2001 field study.

The accuracy of training site selection may be assessed using a bootstrap method. This is done by simply selecting extra training sites (bootstrap sites) that will not be used in the classification. These bootstrap training classes may then be compared to the classification results to evaluate the overall accuracy.

As noted by Jensen (1996), the general rule is that if training data are being extracted from *n* bands, then at least 10*n* pixels of training data are necessary for each class. Four IKONOS bands (blue, green, red, and NIR) were used to extract the training data in this study. Jensen's (1996) recommendation was modified for this study to reflect the small areal extent of Sites #1-3. For the three smaller study sites (Sites #1, #2, and #3), twelve areas of each training class (five training classes) were selected for a total of sixty training sites for burn severity in each study site. Training sites ranged in size between 1 and 1,000 pixels. Ten of the twelve sites were used for classification, and the remaining two were used for a bootstrap method accuracy check. For the larger study site (Site #4), fifty-five areas of each type of training site were selected for a total of two hundred and seventy-five training sites for burn severity. Fifty of the fifty-five sites were used for classification, and the remaining five were used for a bootstrap method accuracy check.

The four classes of burn severity were ranked with the same values as those used in field mapping. High burn severity was ranked with a value of 10, moderate severity was ranked with a value of 9, low burn severity was ranked with a value of 8, and unburned areas were ranked with a value of zero. The training class developed for areas of high reflectance (outcrops, roads, and bare ground) was assigned a value of zero so that these features would not influence the burn severity classifications.

The parallelepiped, spectral angle mapper (SAM), maximum likelihood, and minimum distance algorithms were evaluated to ascertain which classification algorithm yielded results matching closest to field mapping results. The parallelepiped algorithm uses a range of minimum and maximum DN values to classify each pixel in parallelograms fitted over the scatterplot data. This method is computationally simple, but there can be difficulty if training categories overlap. If a pixel value lies above the lower threshold and below the higher threshold for all *n* bands being classified, it is assigned to that class. If the pixel value falls in multiple classes, the pixel is assigned to the last class matched. This algorithm did not provide results similar to field mapping results, possibly due to training category overlap.

The SAM algorithm compares the angle between the endmember spectrum (considered as an *n*-dimensional vector, where *n* is the number of bands) and each pixel vector in *n*-dimensional space. Smaller angles represent closer matches to the reference spectrum. This algorithm uses the spectral pattern of the data rather than the statistical distribution pattern (Sohn and Rebello, 2002). SAM did not predict moderate burn severity appropriately, and all burn severities were overpredicted.

The maximum likelihood algorithm assumes that the statistics for each training class are normally distributed and assigns each pixel to the class that has the highest probability. This is a complex, statistically-based algorithm that requires large computations. No probability threshold was set for this classification. This algorithm yielded slightly better results than the parallelepiped algorithm. It is likely that this algorithm did not provide results similar to field mapping because, in this case, the statistics for each training class are not normally distributed.

The minimum distance algorithm uses the mean vectors of each endmember to calculate the Euclidean distance from each unknown pixel to the mean vector for each class. Pixels are classified to the nearest class. This is a mathematically simple technique but may sometimes be insensitive to different degrees of variance in the data. The maximum standard deviation from the mean and the maximum distance error thresholds were both set to zero. This algorithm provided results in best agreement with the field mapping data. Therefore, this algorithm was used for subsequent analysis. The accuracy of all burn severity classifications was assessed by comparing the bootstrap training sites to the minimum distance classifications (discussed in Section 4.2). Accuracy was also assessed using a pixel-by-pixel statistical comparison of field and remote sensing data, which is discussed in Section 2.4.

Vegetation Cover Assessment

There are several methods of assessing vegetation cover with remote sensing data, including the Composite Burn Index (CBI), the Normalized Burn Ratio (NBR), the Normalized Difference Vegetation Index (NDVI), and the Soil-Adjusted Vegetation Index (SAVI). The CBI is designed to correlate burn severity effects on vegetation as measured in the field to those observed with Landsat TM data (Key and Benson, 1999a). The NBR is a temporal index formulated from Landsat TM bands 4 and 7 and compares temporal indices to discriminate burn characteristics (Key and Benson, 1999b). The NDVI is the difference of the NIR band and the red band divided by the sum of the NIR band and the red band, or (NIR-Red)/(NIR+Red). The SAVI proposed by Huete (1988) is similar to the NDVI with added terms to adjust for different brightnesses of background soil. SAVI is the NDVI multiplied by (1 + L), where L varies between 0-1

depending on the amount of visible soil (note that when L = 0, SAVI = NDVI). When the amount of visible soil in unknown, L = 0.5 is often used. For this study, it is expected that L will vary greatly due to the disparity of burn severities and thus SAVI was not used.

This study utilizes the NDVI to specifically assess vegetation cover displayed by IKONOS data. The NDVI is a widely-used transformation because it is a good indicator of biomass. NDVI values fall between -1 and +1. Higher NDVI values indicate more green vegetation and appear bright. For example, green vegetation generally has NDVI values greater than zero, soils have values close to zero, and water has values less than zero.

In order to determine what NDVI values should represent the ranking values used for understory vegetation cover, NDVI values were compared to field mapping results. These comparisons indicate that study areas with 0-25% understory vegetation cover typically have NDVI values from -1 to -0.5, and thus were assigned a value of 5. Since these areas do not contain water, the low values may be due to the heterogeneous soil cover and ash. Study areas with 26-50% cover have NDVI values between -0.5 and zero, and were assigned a value of 4. Areas with 51-75% cover have NDVI values between zero and 0.5 and were assigned a value of 3. Areas with greater than 75% cover have NDVI values from 0.5 to 1.0 and were assigned a value of 2. NDVI values were imported into ArcMap 8.2 (ESRI, 2002) and reclassified according to these findings. Accuracy was assessed using a pixel-by-pixel statistical comparison of field and remote sensing data, which is discussed in Section 2.4.

GEOGRAPHIC INFORMATION SYSTEM (GIS) STUDY

ArcView 3.3 (ESRI, 2002) was used to create GIS coverages for this study. Coverages were created for each study site and the respective parameters measured in the field, including slope, aspect, burn severity, amount of understory vegetation cover, hydrology, bedrock geology, and soil characteristics. Slope and aspect coverages were developed by using USGS 10-m DEMs rather than by measurements made in the field in order to provide a more comprehensive assessment.

ArcMap 8.2 (ESRI, 2002) was used to convert the GIS coverages from field measurements into raster images. To produce a relative hazard map for landslides, the coverages for slope, aspect, burn severity, hydrology, bedrock geology, and soil characteristics were summed using raster arithmetic. The raster images for slope and aspect were produced with 10-m USGS DEMs, and therefore the arithmetic product has a resolution of 10-m. To produce a relative hazard map for erosion, the sum of these coverages was added to the coverages for understory vegetation cover.

The NDVI transformations and minimum distance classifications were imported into ArcMap 8.2 (ESRI, 2002) and converted to raster images. Unfortunately, there are no soil or fine-resolution hydrology GIS coverages or maps available for the study sites. The 1:100,000-scale geological map that was compiled and digitized specifically for this study was imported to represent the bedrock geology of each site. To produce a relative hazard map for landslides using information not directly obtained from field measurements, raster arithmetic was used to sum the 10-m USGS DEMs for slope and aspect, 4-m minimum distance classifications for burn severity, and the 1:100,000-scale compiled map for bedrock geology. The arithmetic product has a resolution of 10-m (note that the resolution of the geologic map is significantly coarser). To

produce a relative hazard map for erosion, the sum of these coverages was added to the 4-m NDVI raster image for understory vegetation cover.

STATISTICAL COMPARISON OF FIELD AND REMOTE SENSING DATA

The ranking of the parameters derived from field mapping versus remote sensing data were compared by calculating the kappa coefficient, K. K is a measure of association used to describe and test the degree of agreement in classifications (Koch, 1983; Kraemer, 1983). Classification results are grouped into a contingency table to summarize the proportions of correct and incorrect classifications. For example, a simple summary table, known as a 2x2 confusion matrix or error matrix, is as follows:

	Actually Present	Actually Absent
Predicted Present	a	b
Predicted Absent	c	d

where a, b, c, and d represent frequencies of occurrence of possible outcomes from N total outcomes (Welhan, 2003). Actual agreement is indicated by the major diagonal and chance agreement is indicated by the row and column totals (Congalton and Green, 1999). For a 2 x2 confusion matrix, K is defined as:

$$K = \frac{[(a+d) - \{((a+c)(a+b)) + ((b+d)(c+d))\}] / N}{N - [\{((a+c)(a+b)) + ((b+d)(c+d))\}] / N]}$$

Burn severity, vegetation cover, and geology were compared; slope and aspect were not, as these parameters were assessed using the same data source (USGS 10-m DEMs). It is important to note that the final hazard maps were not compared because different parameters could possibly result in the same sum, and thus results would be misleading. For example, an area with high severity burns and no surface water would result in a hazard ranking of 10. This same hazard ranking could also be obtained by an unburned area with surface water.

The field mapping results (and ranking of the specific parameters) are considered the baseline or "accepted" data for the purposes of this study. The remote sensing data was compared to this baseline information. The ranking maps for each of the three parameters for both the landslide and erosion studies at each site were reclassified into values that, when the remote sensing values were subtracted from the field mapping values, would yield unique values (field mapping reclassification values are 25, 50, 75, and 100, and remote sensing reclassification values are 1, 5, 11, and 19) (Table 7). The actual numbers of pixels corresponding to the values in the shaded portion of the table were used to calculate K. The range of K is typically 0-1, with zero corresponding to chance agreement and 1 corresponding to perfect agreement.

Table 7. An example of the 4x4 confusion matrix used to assess the accuracy of the remote sensing burn severity data to field mapping results. The values in the shaded areas will be replaced by the number of pixels corresponding to those values.

		Remote Sensing Reclassification Values			
		1	**5**	**11**	**19**
Field Mapping Reclassification Values	**25**	24	20	14	6
	50	49	45	39	31
	75	74	70	64	56
	100	99	95	89	81

RESULTS

FIELD STUDY AND GIS

Each of the three study sites is approximately one km² and varies in elevation between approximately 1,700-2,600 m. Each site exhibits varying slopes, aspects, burn severity, amount of understory vegetation cover, hydrology, bedrock geology, and soil characteristics. These parameters were mapped in the field during June, July, and August of 2001. Field studies during June, July, and August of 2002 investigated active mass wasting processes and evaluated landslide and erosion hazard susceptibility predictions. The following sections detail the field-based data.

Site #1: Quartzite Mountain

Site #1 is located north of Quartzite Mountain (Figure 2) and covers an area of 0.90 km². Elevation ranges between 2,347-2,621 m. The predominant types of vegetation are Douglas fir and pinegrass.

Parameters

Slope and Aspect

Slopes range between 0-36° (Figure 7) and the predominate aspect is northern (Figure 8).

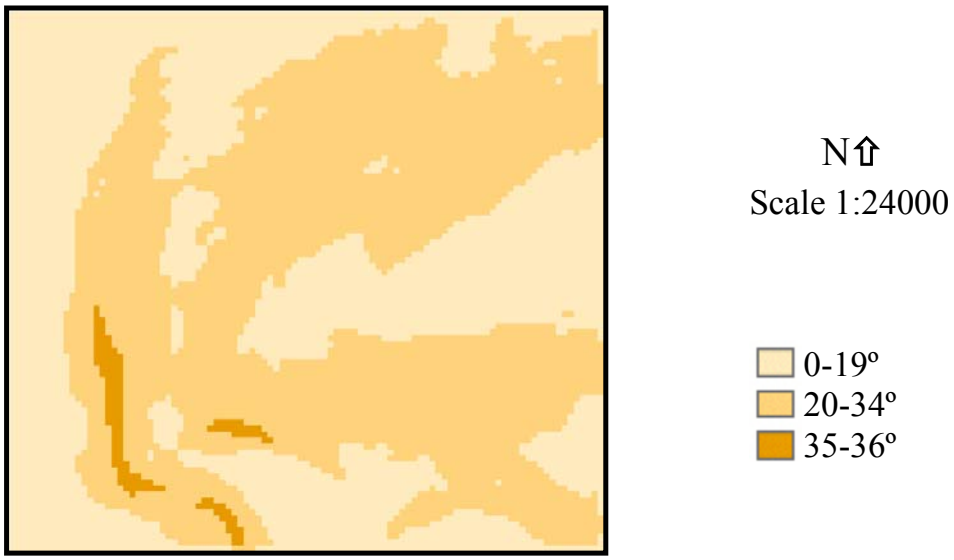

Figure 7. Slopes of Site #1. (Derived from USGS Blackbird Mountain DEM, 10-m resolution.)

Figure 8. Aspects of Site #1. (Derived from USGS Blackbird Mountain DEM, 10-m resolution.)

Burn Severity

The burn intensities of Site #1 include all degrees of severity (Figure 9). High severity burns, ranked with a value of 10 for this study, cover 80% of the total site area. Moderate severity burns were ranked with a value of 9 and cover 8% of the site. Low severity burns were ranked with a value of 8 and cover 9% of the site. A small area of the site, 3%, is unburned and was ranked with a value of zero.

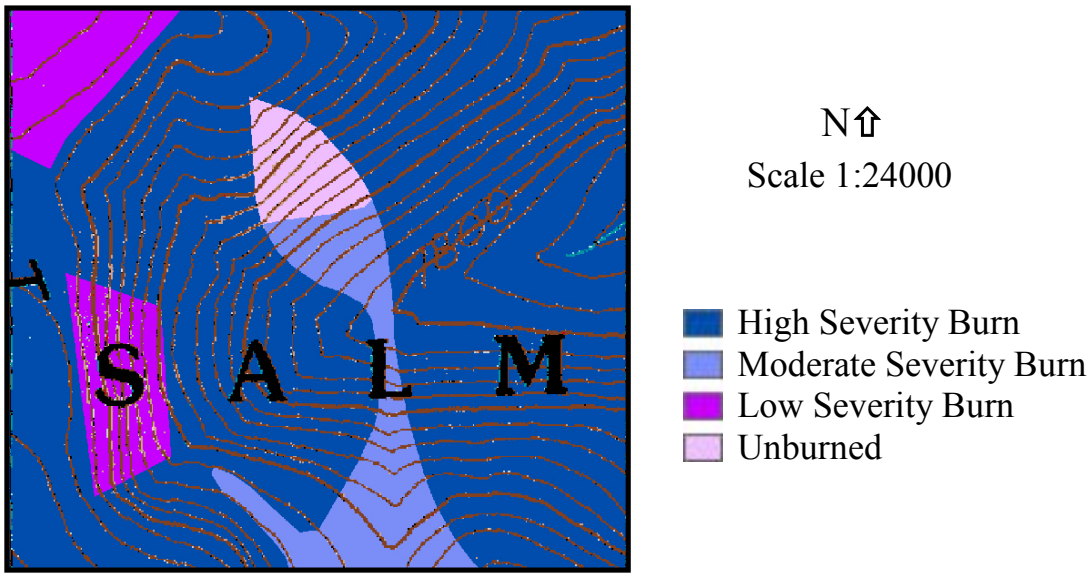

Figure 9. Burn severities of Site #1. (Base map from USGS Blackbird Mountain 7.5 Minute Quadrangle.)

Understory Vegetation Cover

Most of this site, 81% of the total area, has 0-25% understory vegetation cover (Figure 10). These areas were ranked with a value of 5. The remaining 19% of the area has greater than 75% cover, and was ranked with a value of 2.

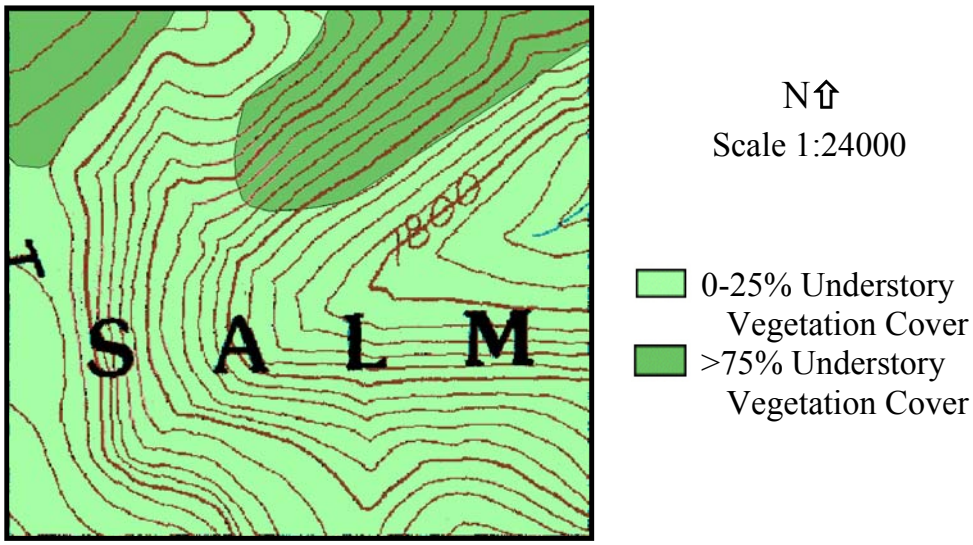

Figure 10. Understory vegetation cover of Site #1. (Base map from USGS Blackbird Mountain 7.5 Minute Quadrangle.)

Hydrology

A large percentage of this site, 96%, contains no surface water (Figure 11). These areas were ranked with a value of zero. Only 4% of the site has surface water, which is in the form of small springs that originate in the south and west portions of the site and feed into a small creek at the east side of the site. These areas were ranked with a value of 10.

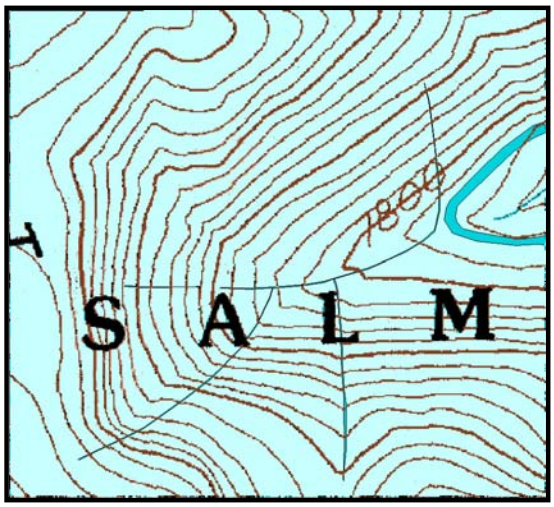

Figure 11. Hydrology of Site #1. (Base map from USGS Blackbird Mountain 7.5 Minute Quadrangle.)

Geology

The bedrock in most of the study area consists of west-dipping thin-bedded microlaminated fine-grained sandstone (Figure 12). These rocks are mapped as "type" or "lower" Yellowjacket Formation by Ekren (1988) and Tysdal (2000). Winston et al. (1999) mapped these units as the argillaceous quartzite unit of Ekren (1988) which lies stratigraphically above the Hoodoo Quartzite. In the southeast portion of the study area, the bedrock consists of west-dipping thin-bedded siltite and fine-grained sandstone with characteristic convoluted cracks in silt filled with fine sand. These rocks are identical to outcrops of the Wallace Formation along the Salmon River and are mapped as Apple Creek Formation by Tysdal (2000). A south-dipping normal fault mapped by Tysdal (2000) runs along the prominent gully in the southeast part of the study area and separates the two stratigraphic units. As this site is primarily composed of cohesive sandstones and siltstones, it was ranked with a value of 1.

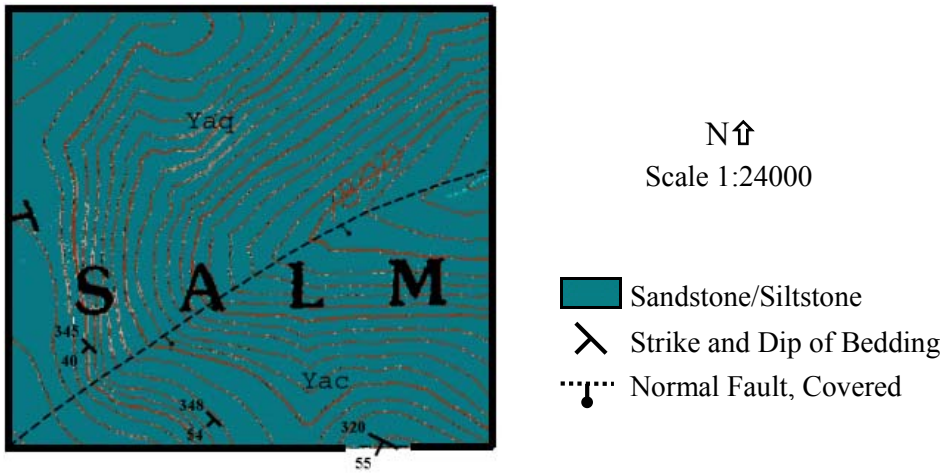

Figure 12. Geology of Site #1. A south-dipping normal fault runs along the prominent gully and separates fine-grained sandstone (Yaq) from siltite and fine-grained sandstone (Yac). (Base map from USGS Blackbird Mountain 7.5 Minute Quadrangle.)

Soil Characteristics
All of the soil evaluated in this site is sandy silt, which was assigned a value of 5 (Figure 13).

Landslide and Erosion Hazard Ranking
The relative hazard map for landslides incorporates the parameters of slope, aspect, burn severity, hydrology, bedrock geology, and soil characteristics. The relative values for landslide hazard range between 9-31, with 9 being relatively less likely to experience landslides and 31 being more likely (Figure 14). Small areas with high values occur in the southern and northeastern portion of the site. The northern portion of this site has a large area with moderately high values.

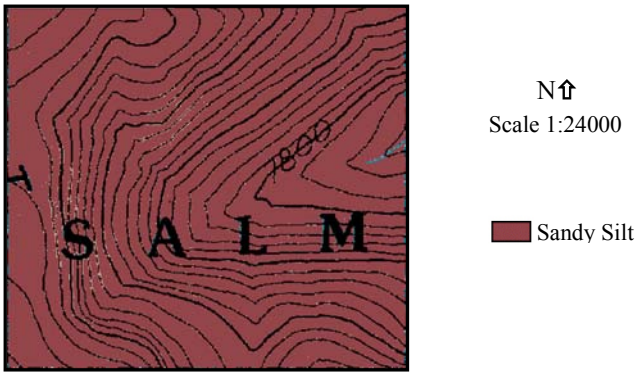

Figure 13. Soil type of Site #1. (Base map from USGS Blackbird Mountain 7.5 Minute Quadrangle.)

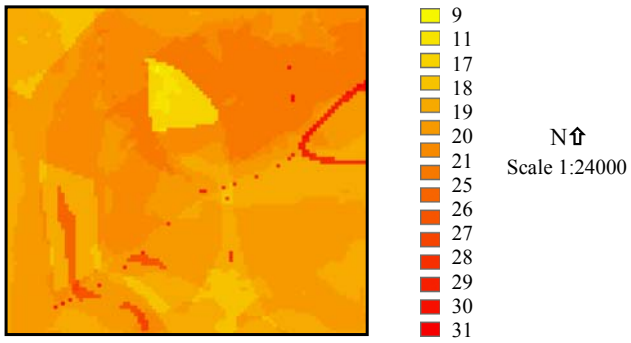

Figure 14. Relative landslide hazard for Site #1. Areas relatively more likely to experience landslides have higher values. (Derived from USGS Blackbird Mountain DEM, 10-m resolution.)

The relative hazard map for erosion incorporates the parameters of slope, aspect, burn severity, understory vegetation cover, hydrology, bedrock geology, and soil characteristics. The relative values for erosion hazard range between 12-40, with 12 being relatively less likely to experience erosion and 40 being more likely (Figure 15). Small areas with high values occur in the southwestern and northeastern portion of the site. The southeastern portion of this site has a large area with moderately high values.

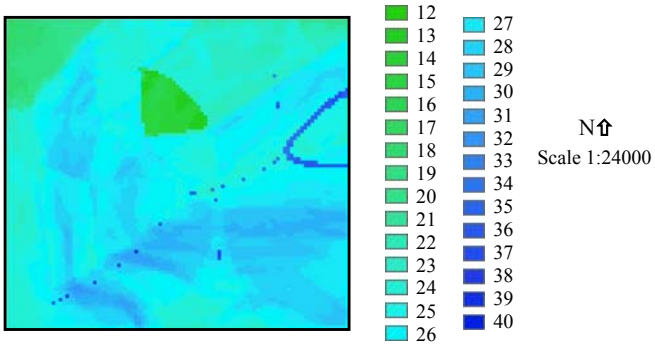

Figure 15. Relative erosion hazard for Site #1. Areas relatively more likely to experience erosion have higher values. (Derived from USGS Blackbird Mountain DEM, 10-m resolution.)

Site #2: Fourth of July Creek

Site #2 is located south of Fourth of July Creek (Figure 2) and covers an area of 1.2 km². Elevation ranges between 2,134-2,438 m. The predominant types of vegetation are Douglas Fir and pinegrass.

Parameters

Slope and Aspect

Slopes range from 1-39° (Figure 16) and aspects are predominantly eastern and western (Figure 17).

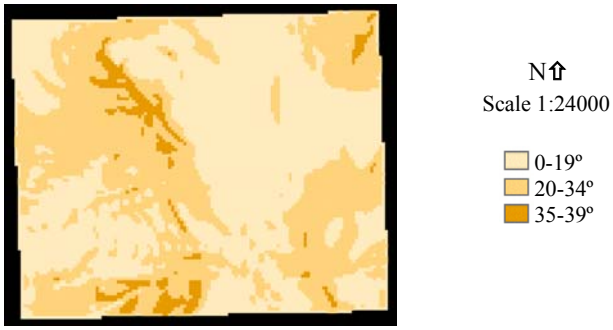

Figure 16. Slopes of Site #2. (Derived from USGS Duck Creek Point DEM, 10-m resolution.)

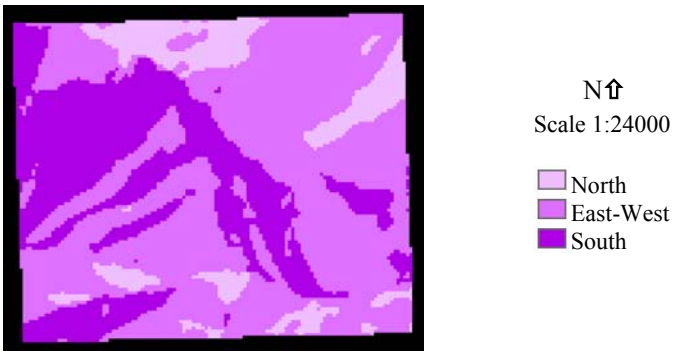

Figure 17. Aspects of Site #2. (Derived from USGS Duck Creek Point DEM, 10-m resolution.)

Burn Severity

The burn intensities of Site #2 include all degrees of severity (Figure 18). High severity burns, ranked with a value of 10 for this study, cover 25% of the total site area. Moderate severity burns were ranked with a value of 9 and cover 32% of the site. Low severity burns were ranked with a value of 8 and cover 14% of the site. Unburned areas cover 29% of the site area and were ranked with a value of zero.

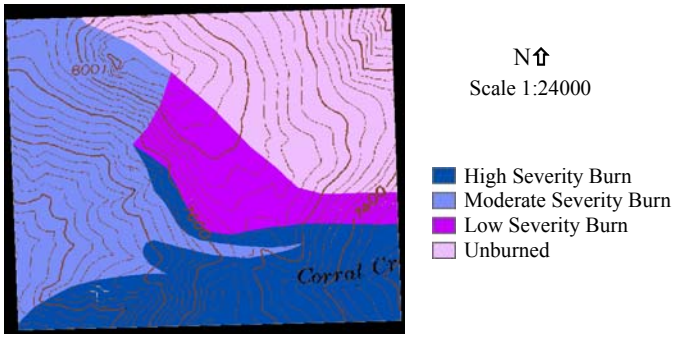

Figure 18. Burn severities of Site #2. (Base map from USGS Duck Creek Point 7.5 Minute Quadrangle.)

Understory Vegetation Cover

A small area comprising 5% of the total site area has 0-25% understory vegetation cover and was ranked with a value of 5. Another 27% of the site area has 26-50% cover and was assigned a value of 4. The remaining 68% of the total area has greater than 75% cover and was ranked with a value of 2 (Figure 19).

Hydrology

This particular site contains no surface water, and was thus ranked with a value of zero (Figure 20).

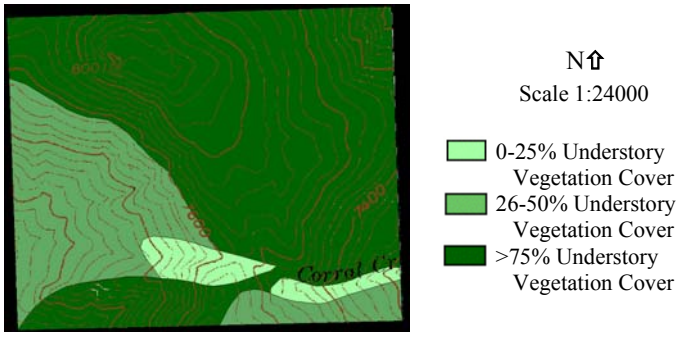

Figure 19. Understory vegetation cover of Site #2. (Base map from USGS Duck Creek Point 7.5 Minute Quadrangle.)

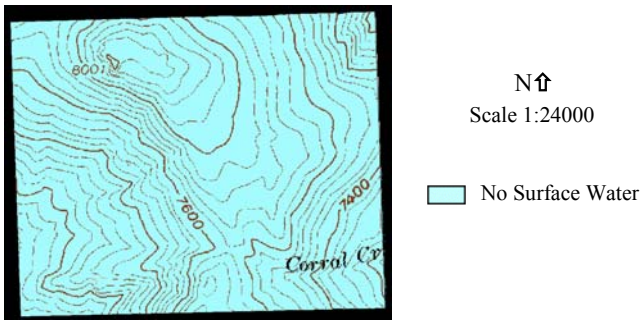

Figure 20. Hydrology of Site #2. (Base map from USGS Duck Creek Point 7.5 Minute Quadrangle.)

Geology

The geology of this area consists of the Challis Volcanic Group within the Panther Creek graben, including epiclastic bedded lapilli tuffs, welded tuffs, and minor rhyolite lavas (Figure 21). As noted by Fisher et al. (1995), the study area is underlain by east-dipping strata assigned to units consisting of flow-layered rhyolite. This site was ranked with a value of 4, as this lithology is considerably more friable than any other lithologies investigated in this study.

Soil Characteristics

Clayey silt and sandy silt cover 25% of the site (Figure 22). Although both soils are predominantly silt, the clay component makes the clayey silt slightly more cohesive and thus less easily entrained. The sand component of the sandy silt makes the soil grain size slightly larger overall and also less easily entrained; however, the sand component may increase the infiltration capacity of the soil slightly. Taking all of these variables into consideration, the clayey silt and the sandy silt were both ranked with a value of 5. Silty sand covers the remaining 75% of the site and was assigned a value of 4.

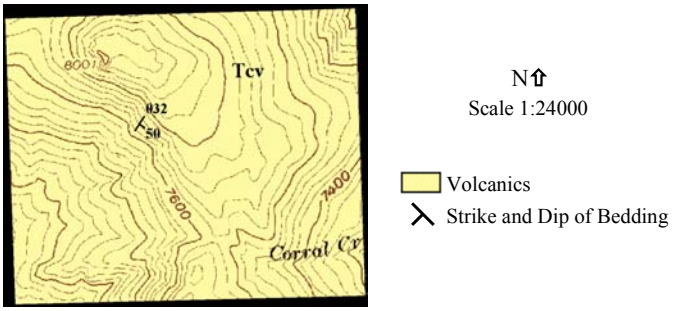

Figure 21. Geology of Site #2. This site consists of the Challis Volcanic Group (Tcv), including epiclastic bedded lapilli tuffs, welded tuffs, and minor rhyolite lavas. (Base map from USGS Duck Creek Point 7.5 Minute Quadrangle.)

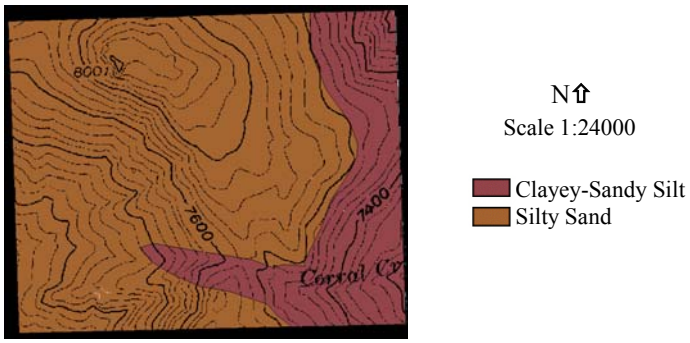

Figure 22. . Soil type of Site #2. (Base map from USGS Duck Creek Point 7.5 Minute Quadrangle).

Landslide and Erosion Hazard Ranking

The relative hazard map for landslides incorporates the parameters of slope, aspect, burn severity, hydrology, bedrock geology, and soil characteristics. Relative values for landslide hazard range between 10-31, with 10 being relatively less likely to experience landslides and 31 being more likely (Figure 23). The highest values occur in the southern and northwest portions of the site.

The relative hazard map for erosion incorporates the parameters of slope, aspect, burn severity, understory vegetation cover, hydrology, bedrock geology, and soil characteristics. The relative values for erosion hazard range between 11-34, with 11 being relatively less likely to experience erosion and 34 being more likely (Figure 24). The highest values occur in the southern and northwestern portions of the site.

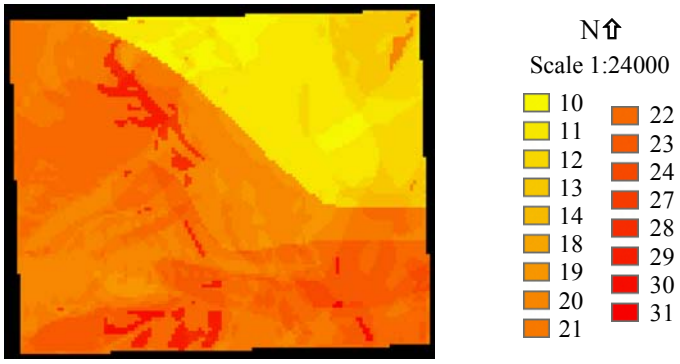

Figure 23. Relative landslide hazard for Site #2. Areas relatively more likely to experience landslides have higher values. (Derived from USGS Duck Creek Point DEM, 10-m resolution).

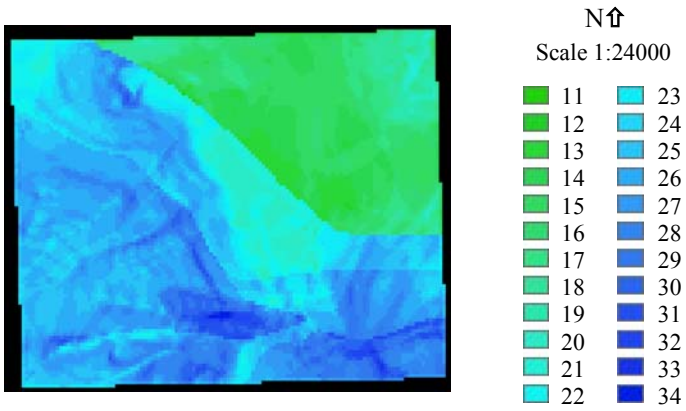

Figure 24. Relative erosion hazard for Site #2. Areas relatively more likely to experience erosion have higher values. (Derived from USGS Duck Creek Point DEM, 10-m resolution).

Site #3: Lake Creek

Site #3 is located west of Lake Creek (Figure 2) and covers an area of 0.95 km². Elevation ranges between 1,707-2,195 m. The predominant types of vegetation are Douglas fir, ponderosa pine, pinegrass, and bunch grass.

Parameters

Slope and Aspect

Slopes range from 0-56° (Figure 25) and the predominant aspect is eastern (Figure 26).

Figure 25. Slopes of Site #3. (Derived from USGS Yellowjacket DEM, 10-m resolution).

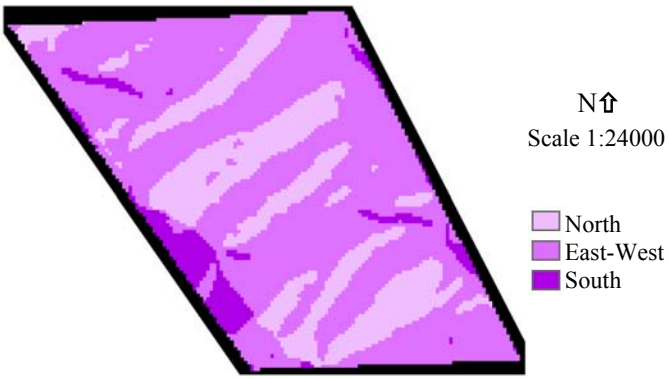

Figure 26. Aspects of Site #3. (Derived from USGS Yellowjacket DEM, 10-m resolution).

Burn Severity
High severity burns cover 50% of Site #3 and were ranked with a value of 10 (Figure 27). Moderate severity burns were ranked with a value of 9 and cover 19% of the site. Low severity burns were ranked with a value of 8 and cover 4% of the site. Unburned areas cover 27% of the site area and were ranked with a value of zero.

Understory Vegetation Cover
Approximately 14% of the site area has 26-50% cover and was assigned a value of 4 (Figure 28). Another 20% of the site area has 51-75% cover and was assigned a value of 3. The remaining 66% of the site has greater than 75% cover, and was ranked with a value of 2.

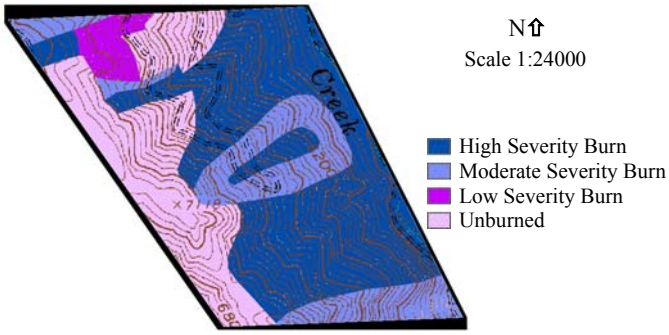

Figure 27. Burn severities of Site #3. (Base map from USGS Yellowjacket 7.5 Minute Quadrangle).

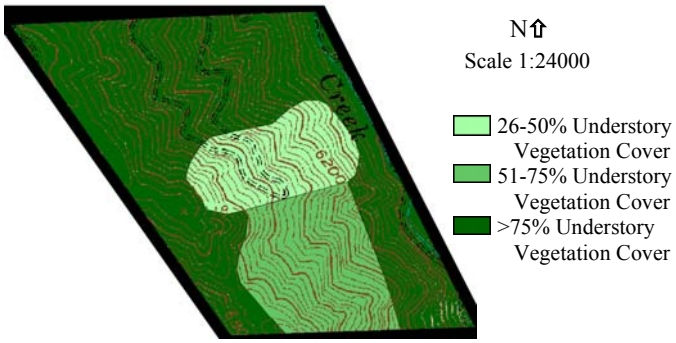

Figure 28. Understory vegetation cover of Site #3. (Base map from USGS Yellowjacket 7.5 Minute Quadrangle).

Hydrology
A large percentage of this site, 98%, contains no surface water (Figure 29). These areas were ranked with a value of zero. Only 2% of the site has surface water, which is in the form of a stream (Lake Creek) along the eastern perimeter of the site, and was ranked with a value of 10.

Figure 29. Hydrology of Site #3. (Base map from USGS Yellowjacket 7.5 Minute Quadrangle).

Geology

The bedrock of this site is primarily coarse-grained granodiorite (mapped by Ekren (1988) as Ordovician in age) and was ranked with a value of 2 (Figure 30). A ridge at the western portion of the site is intruded by northeast-trending dikes mapped as quartz porphyry intrusions of the Challis Volcanics and thus ranked with a value of 4.

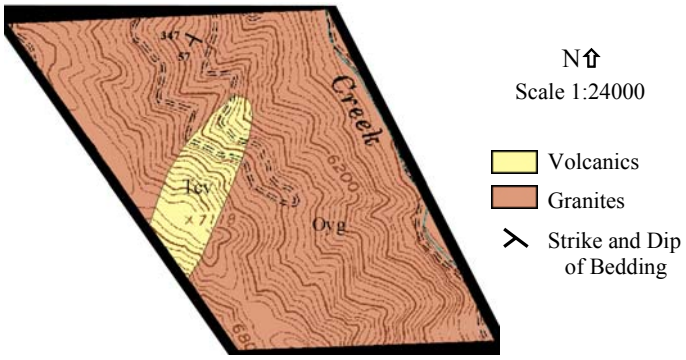

Figure 30. Geology of Site #3. The bedrock of this site is primarily coarse-grained granodiorite (Oyg). A ridge at the western portion of the site is intruded by northeast-trending dikes of quartz porphyry intrusions (Tcv). (Base map from USGS Yellowjacket 7.5 minute quadrangle).

Soil Characteristics

Approximately 83% of the soil evaluated in this site is silty sand, which was assigned a value of 4 (Figure 31). The remaining 17% of the soil is clayey-sandy silt and was assigned a value of 5.

Landslide and Erosion Hazard Ranking

The relative hazard map for landslides incorporates the parameters of slope, aspect, burn severity, hydrology, bedrock geology, and soil characteristics. Relative values for landslide hazard range between 8-30, with 8 being relatively less likely to experience landslides and 30 being more likely (Figure 32). The highest values occur in the central and eastern portions of the site.

Figure 31. Soil type of Site #3. (Base map from USGS Yellowjacket 7.5 Minute Quadrangle).

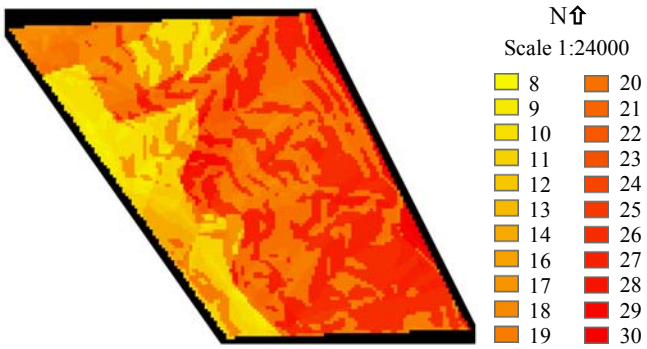

Figure 32. Relative landslide hazard for Site #3. Areas relatively more likely to experience landslides have higher values. (Derived from USGS Yellowjacket DEM, 10-m resolution).

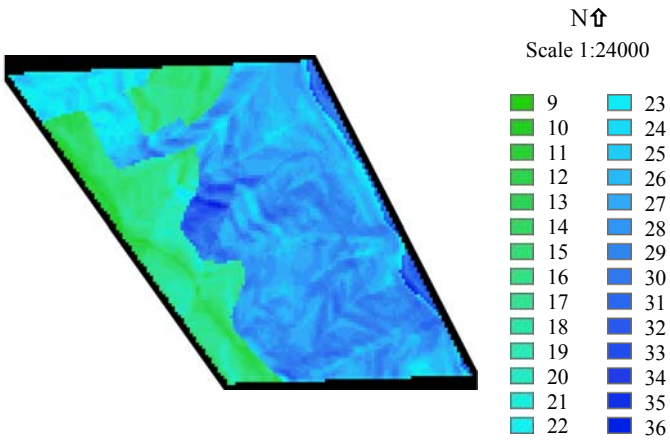

Figure 33. Relative erosion hazard for Site #3. Areas relatively more likely to experience erosion have higher values. (Derived from USGS Yellowjacket DEM, 10-m resolution).

The relative hazard map for erosion incorporates the parameters of slope, aspect, burn severity, understory vegetation cover, hydrology, bedrock geology, and soil characteristics. The relative values for erosion hazard range between 9-36, with 9 being relatively less likely to experience erosion and 36 being more likely (Figure 33). The highest values occur in the central and eastern portions of the site.

REMOTE SENSING STUDY AND GIS

Burn severity and amount of vegetation cover were analyzed for Sites #1-4 using IKONOS imagery. Burn severity was assessed using a minimum distance algorithm and vegetation cover was assessed using an NDVI transformation. As previously stated, there are no soil or fine-resolution hydrology GIS coverages or maps available for the study sites; therefore, soil characteristics and hydrology were not evaluated by remote sensing or GIS methods. Pre-existing geological maps were digitized to provide bedrock geology coverage for this aspect of the study. USGS 10-m DEM's provided slope and aspect coverages. Therefore, the parameters evaluated with remote sensing data include slope, aspect, burn severity, vegetation cover (for erosion only), and geology.

The accuracy of remote sensing image interpretations for Sites #1-3 was evaluated by comparing them to field mapping results. The accuracy of remote sensing image interpretations for Site #4 could only be evaluated by comparing interpretations at Sites #1-3 (within Site #4) to results obtained from field mapping results.

Site #1: Quartzite Mountain

Parameters

Burn Severity

The burn intensities of Site #1 include all degrees of severity (Figure 34). High severity burns, ranked with a value of 10 for this study, cover 65% of the total site area. Moderate severity burns were ranked with a value of 9 and cover 18% of the site. Low severity burns were ranked with a value of 8 and cover 6% of the site. A small area of the site, 4%, is unburned and was ranked with a value of zero. About 7% of the site are areas of rock outcrops/roads and high reflectance and were ranked with a value of zero.

Vegetation Cover

The NDVI values for this site range from -0.220 to 0.657. Approximately 30% of this site has 26-50% vegetation cover (Figure 35). These areas were ranked with a value of 4. Most of the site, 69% of the total area, has 51-75% cover, and was ranked with a value of 3. The remaining 1% of the area has greater than 75% cover and was ranked with a value of 2.

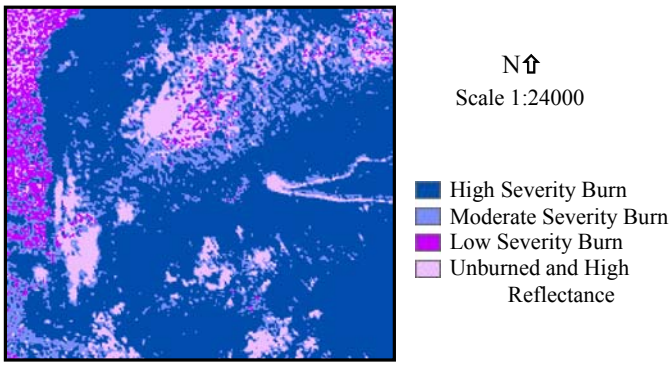

Figure 34. Burn severity of Site #1 assessed with a minimum distance algorithm. Areas of high reflectance include rock outcrops and roads. (Derived from IKONOS imagery, 4-m resolution).

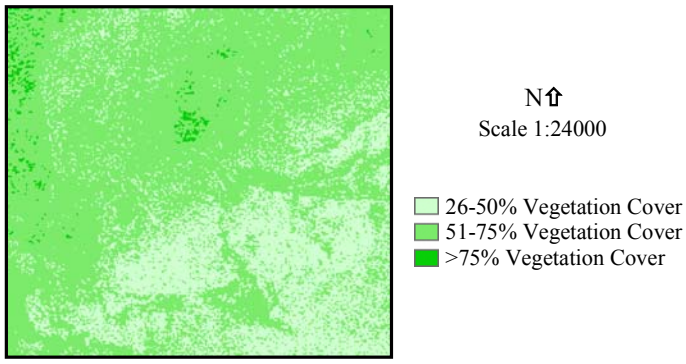

Figure 35. Vegetation cover of Site #1 assessed with an NDVI transformation. (Derived from IKONOS imagery, 4-m resolution).

Geology

The digitized map agrees with field mapping in that this site is primarily composed of sandstones and siltstones (Figure 12). This site was thus ranked with a value of 1.

Landslide and Erosion Hazard Ranking

The relative hazard map for landslides incorporates the parameters of slope, aspect, burn severity, and bedrock geology. The relative values for landslide hazard range between 3-22, with 3 being relatively less likely to experience landslides and 22 being more likely (Figure 36). The highest values occur in the southwest and northern portions of the site.

The relative hazard map for erosion incorporates the parameters of slope, aspect, burn severity, vegetation cover, and bedrock geology. The relative values for erosion hazard range between 4-26, with 4 being relatively less likely to experience erosion and 26 being more likely (Figure 37). The highest values occur in the southern and southwest portions of the site.

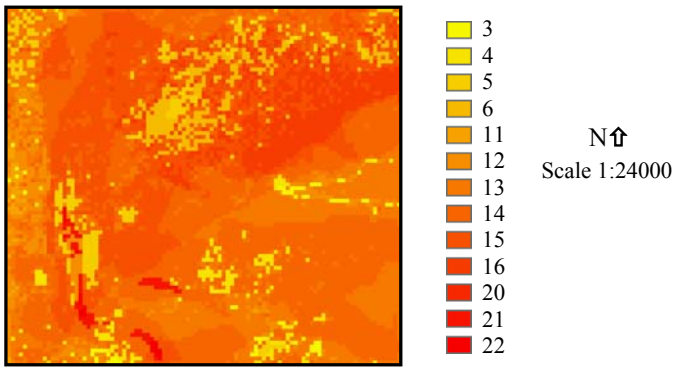

Figure 36. Relative landslide hazard for Site #1. Areas relatively more likely to experience landslides have higher values. (Derived from USGS Blackbird Mountain DEM, 10-m resolution, and IKONOS imagery, 4-m resolution).

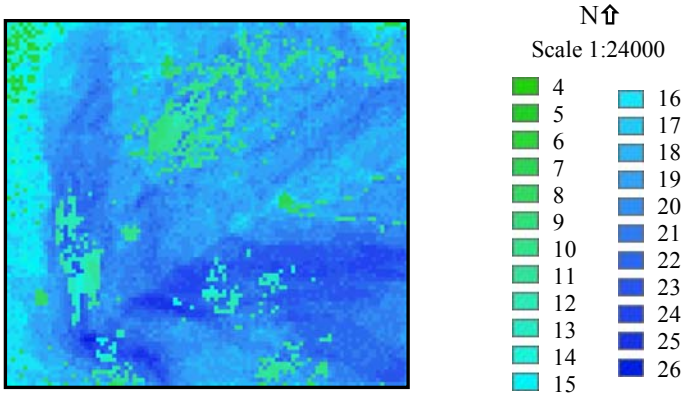

Figure 37. Relative erosion hazard for Site #1. Areas relatively more likely to experience erosion have higher values. (Derived from USGS Blackbird Mountain DEM, 10-m resolution, and IKONOS imagery, 4-m resolution).

Site #2: Fourth of July Creek

Parameters

Burn Severity

The burn severities of Site #2 include all degrees (Figure 38). High severity burns, ranked with a value of 10 for this study, cover 23% of the total site area. Moderate severity burns were ranked with a value of 9 and cover 27% of the site. Low severity burns were ranked with a value of 8 and cover 27% of the site. A small area of the site, 19%, is unburned and ranked with a value of zero. About 4% of the site are areas of rock outcrops/roads and high reflectance and were ranked with a value of zero.

Vegetation Cover

The NDVI values for this site range from -0.207 to 0.692. Approximately 3% of the site area has 26-50% vegetation cover and was ranked with a value of 4 (Figure 39). Most of this site, 79% of the total area, has 51-75% vegetation cover. These areas were ranked with a value of 3. The remaining 18% of the area has greater than 75% cover and was ranked with a value of 2.

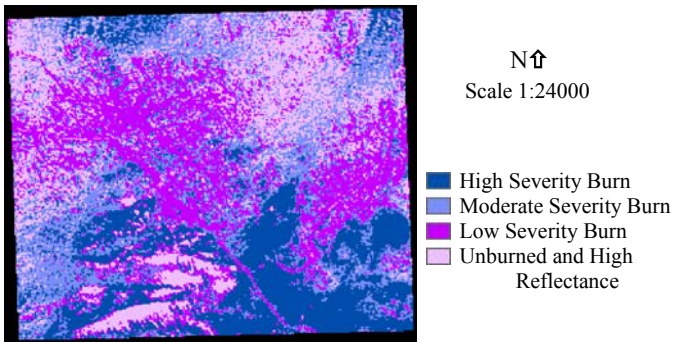

Figure 38. Burn severity of Site #2 assessed with a minimum distance algorithm. Areas of high reflectance include rock outcrops and roads. (Derived from IKONOS imagery, 4-m resolution).

Geology

The digitized map agrees with field mapping in that this site primarily consists of the Challis Volcanic Group and was thus ranked with a value of 3 (Figure 21).

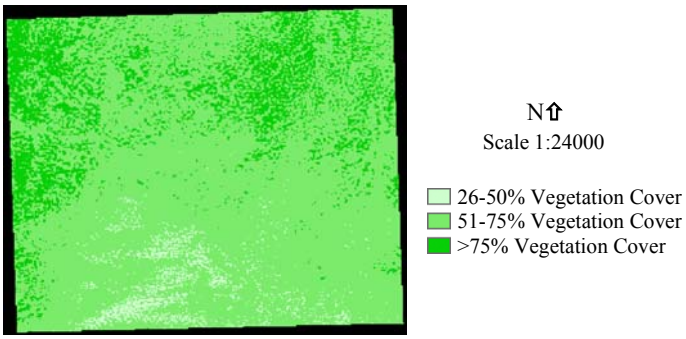

Figure 39. Vegetation cover of Site #2 assessed with an NDVI transformation. (Derived from IKONOS imagery, 4-m resolution).

Landslide and Erosion Hazard Ranking

The relative hazard map for landslides incorporates the parameters of slope, aspect, burn severity, and bedrock geology. The relative values for landslide hazard range between 6-26, with 6 being relatively less likely to experience landslides and 26 being more likely (Figure 40). The highest values occur in the southwest, northeast, and northwest portions of the site.

The relative hazard map for erosion incorporates the parameters of slope, aspect, burn severity, vegetation cover, and bedrock geology. The relative values for erosion hazard range between 7-28, with 7 being relatively less likely to experience erosion and 28 being more likely (Figure 41). The highest values occur in the southwest, northeast, and northwest portions of the site.

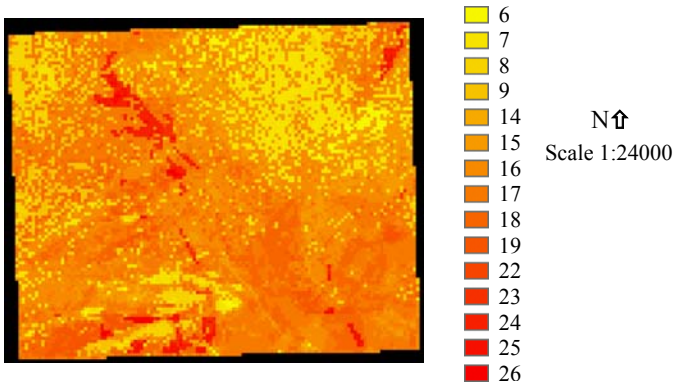

Figure 40. Relative landslide hazard for Site #2. Areas relatively more likely to experience landslides have higher values. (Derived from USGS Blackbird Mountain DEM, 10-m resolution, and IKONOS imagery, 4-m resolution).

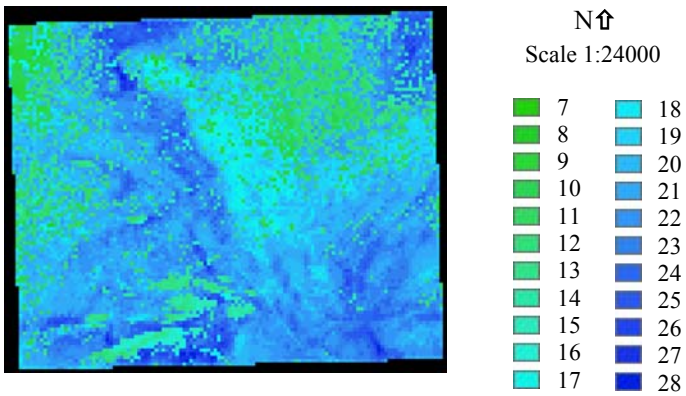

Figure 41. Relative erosion hazard for Site #2. Areas relatively more likely to experience erosion have higher values. (Derived from USGS Blackbird Mountain DEM, 10-m resolution, and IKONOS imagery, 4-m resolution).

Site #3: Lake Creek

Parameters

Burn Severity

The burn intensities of Site #3 include all degrees of severity (Figure 42). High severity burns, ranked with a value of 10 for this study, cover 32% of the total site area. Moderate severity burns were ranked with a value of 9 and cover 17% of the site. Low severity burns were ranked with a value of 8 and cover 27% of the site. A small area of the site, 19%, is unburned and thus ranked with a value of zero. About 5% of the site are areas of rock outcrops/roads and high reflectance and were ranked with a value of zero.

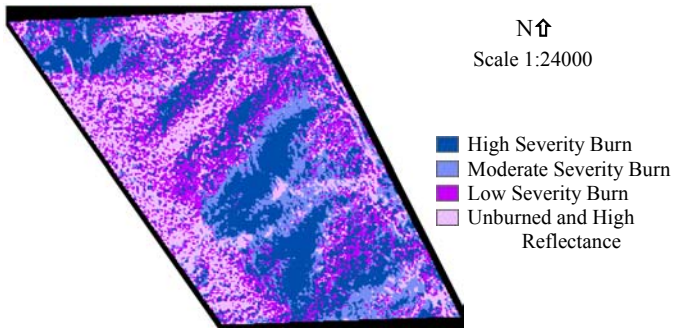

Figure 42. Burn severity of Site #3 assessed with a minimum distance algorithm. Areas of high reflectance include rock outcrops and roads. (Derived from IKONOS imagery, 4-m resolution).

Vegetation Cover

The NDVI values for this site range from -0.309 to 0.710. Most of this site, 85% of the total area, has 51-75% vegetation cover (Figure 43). These areas were ranked with a value of 3. Approximately 3% of the site area has 26-50% vegetation cover and was ranked with a value of 4. The remaining 12% of the area has greater than 75% cover and was ranked with a value of 2.

Geology

The bedrock of this site is primarily coarse-grained granodiorite (mapped by Ekren as Ordovician in age) which was ranked with a value of 2 (Figure 44). The digitized map shows a large area covered by northeast-trending quartz porphyry intrusions (ranked with a value of 4), larger than the area indicated by field mapping. The digitized map also shows an area of granite in the northwest corner not indicated by field mapping; however, this granite was ranked with the same value (2) as the granodiorite and thus not distinguished on the map.

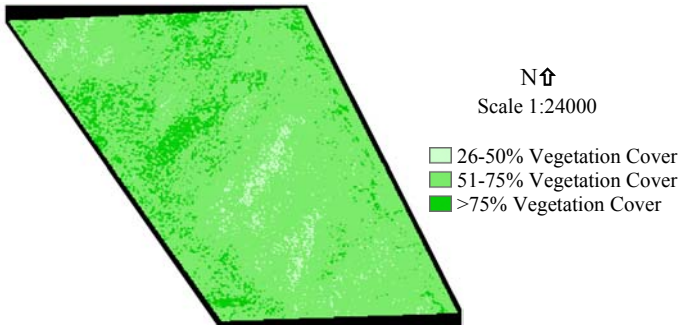

Figure 43. Vegetation cover of Site #3 assessed with an NDVI transformation. (Derived from IKONOS imagery, 4-m resolution).

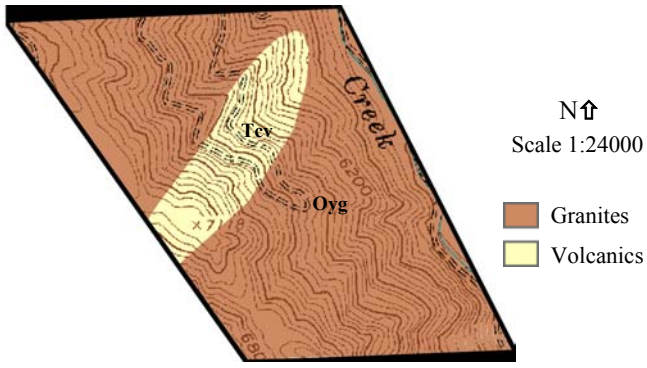

Figure 44. Geology of Site #3. The bedrock of this site is primarily coarse-grained granodiorite (Oyg). A ridge at the western portion of the site is intruded by northeast-trending dikes of quartz porphyry intrusions (Tcv). No attitudes available on source map.

Landslide and Erosion Hazard Ranking

The relative hazard map for landslides incorporates the parameters of slope, aspect, burn severity, and bedrock geology. The relative values for landslide hazard range between 3-25, with 3 being relatively less likely to experience landslides and 25 being more likely (Figure 45). The highest values occur in the eastern two-thirds of the site.

The relative hazard map for erosion incorporates the parameters of slope, aspect, burn severity, vegetation cover, and bedrock geology. The relative values for erosion hazard range between 5-29, with 5 being relatively less likely to experience erosion and 29 being more likely (Figure 46). The highest values occur in the eastern two-thirds of the site.

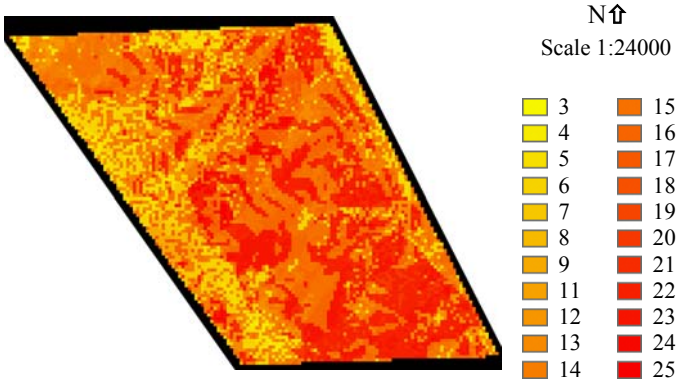

Figure 45. Relative landslide hazard for Site #3. Areas relatively more likely to experience landslides have higher values. (Derived from USGS Blackbird Mountain DEM, 10-m resolution, and IKONOS imagery, 4-m resolution).

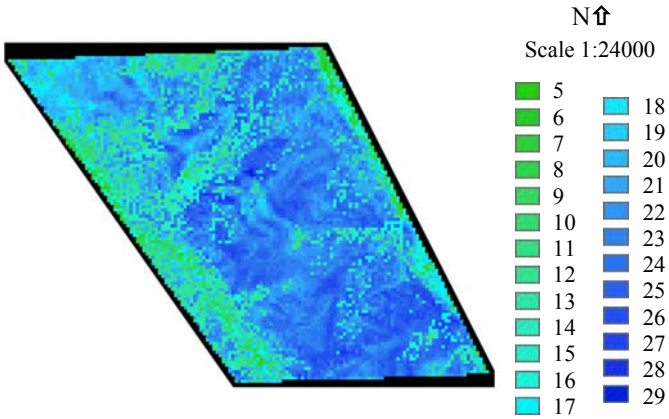

Figure 46. Relative erosion hazard for Site #3. Areas relatively more likely to experience erosion have higher values. (Derived from USGS Blackbird Mountain DEM, 10-m resolution, and IKONOS imagery, 4-m resolution).

Site #4: Salmon-Challis National Forest

Parameters

The parameters evaluated for Site #4 include slope, aspect, burn severity, vegetation cover (for erosion only), and geology. These are the same parameters used to evaluate Sites #1-3 with remote sensing data.

Slope and Aspect

Slopes range between 0-75° (Figure 47) and the predominate aspects are eastern and western (Figure 48).

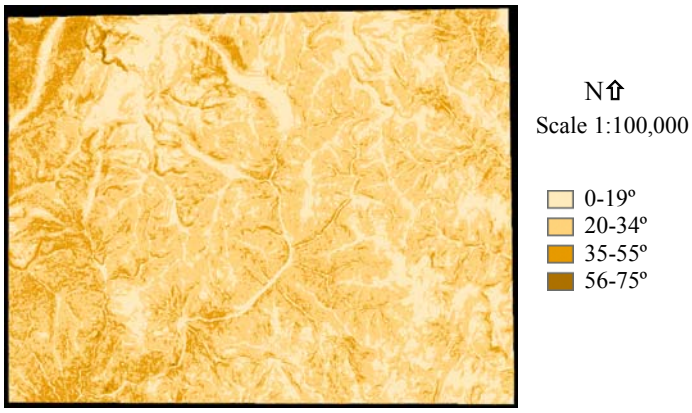

Figure 47. Slopes of Site #4. (Derived from the following USGS DEMs, 10-m resolution: Hoodoo Meadows, Blackbird Mountain, Blackbird Creek, Opal Lake, Duck Creek Point, and Yellowjacket).

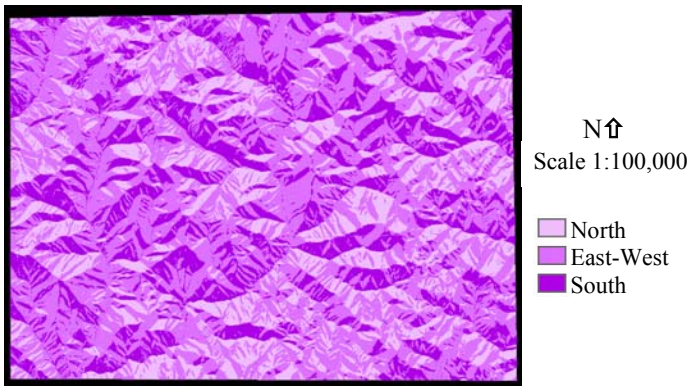

Figure 48. Aspects of Site #4. (Derived from the following USGS DEMs, 10-m resolution: Hoodoo Meadows, Blackbird Mountain, Blackbird Creek, Opal Lake, Duck Creek Point, and Yellowjacket).

Burn Severity

The burn intensities of Site #4 include all degrees of severity (Figure 49). High severity burns, ranked with a value of 10 for this study, cover 11% of the total site area. Moderate severity burns were ranked with a value of 9 and cover 12% of the site. Low severity burns were ranked with a value of 8 and cover 45% of the site. The remaining 25% of the total site area is unburned and ranked with a value of zero. About 7% of the site are areas of rock outcrops/roads and high reflectance and were ranked with a value of zero.

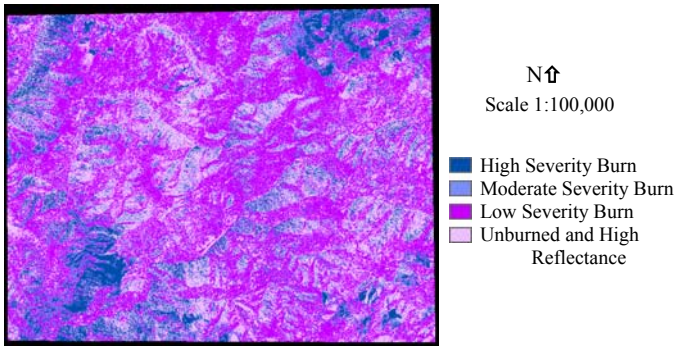

Figure 49. Burn severities of Site #4 assessed with a minimum distance algorithm. Areas of high reflectance include rock outcrops and roads. (Derived from IKONOS imagery, 4-m resolution).

Vegetation Cover

The NDVI values for this site range from -1.0 to 0.767. Most of this site, 78% of the total area, has 51-75% vegetation cover (Figure 50). These areas were ranked with a value of 3. Approximately 21% of the area has greater than 75% cover and was ranked with a value of 2. Only 1% of the site area has 26-50% vegetation cover and was ranked with a value of 4, and less than 1% of the area has 0-25% cover and was ranked with a value of 5.

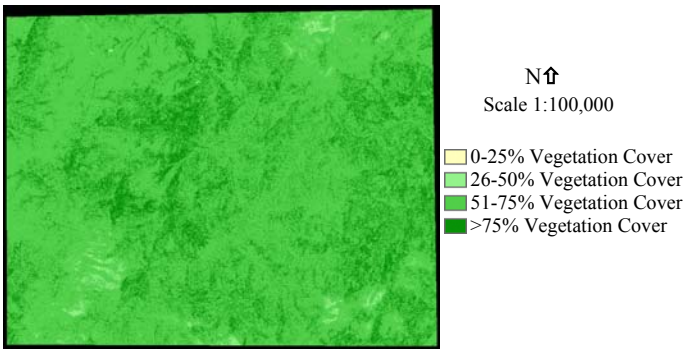

Figure 50. Vegetation cover of Site #4 assessed with an NDVI transformation. (Derived from IKONOS imagery, 4-m resolution).

Geology

There are seven types of bedrock in this site (Figure 51). Units assigned a ranking value of 1 include the Type Yellowjacket Formation, the Hoodoo Quartzite, and the informal argillaceous member of the Cobalt Yellowjacket Formation. Units assigned a ranking value of 2 include the Ordovician or Middle Proterozoic granites, the granitic rocks of the Idaho Batholith, and the Tertiary granites of the Casto and Crags Plutons. The Challis Volcanic Group and minor areas of Quaternary alluvium were ranked with a value of 4.

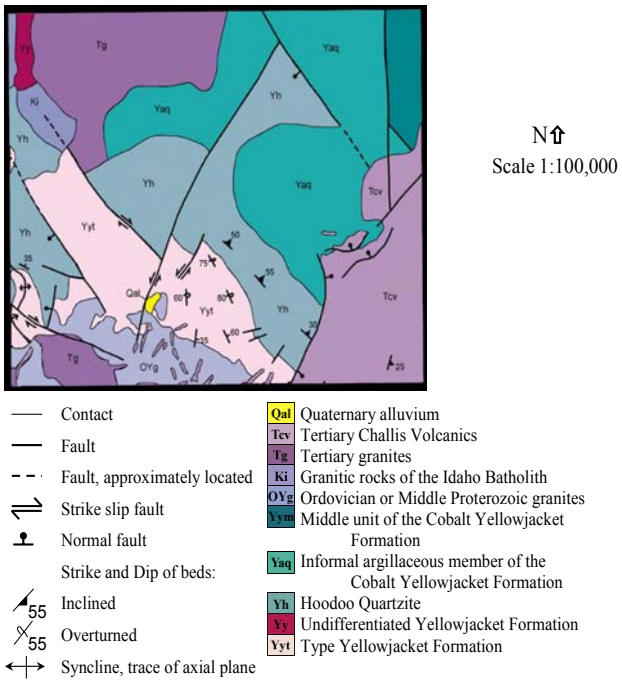

Figure 51. Geology of Site #4. The bedrock of this site consists of seven main bedrock types and Quaternary alluvium. (Source map from compiled from Ross (1934), Ekren (1988), Evans and Connor (1993), and Winston et al. (1999)).

Landslide and Erosion Hazard Ranking

The relative hazard map for landslides incorporates the parameters of slope, aspect, burn severity, and bedrock geology. The relative values for landslide hazard range between 3-27,

with 3 being relatively less likely to experience landslides and 27 being more likely (Figure 52). The highest values occur in the northwestern and southwestern portions of the site.

The relative hazard map for erosion incorporates the parameters of slope, aspect, burn severity, vegetation cover, and bedrock geology. The relative values for erosion hazard range between 4-31, with 4 being relatively less likely to experience erosion and 31 being more likely (Figure 53). The highest values also occur in the northwestern and southwestern portions of the site.

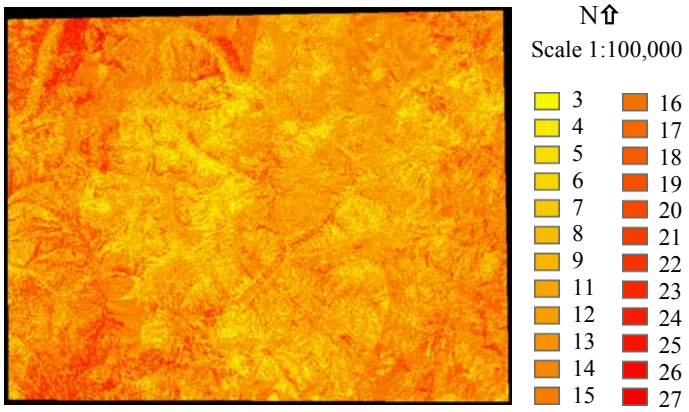

Figure 52. Relative landslide hazard for Site #4. Areas relatively more likely to experience landslides have higher values. (Derived from USGS Blackbird Mountain DEM, 10-m resolution, and IKONOS imagery, 4-m resolution).

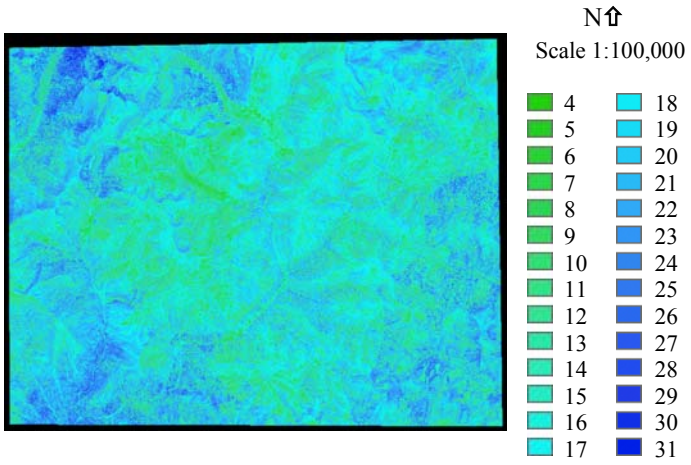

Figure 53. Relative erosion hazard for Site #4. Areas relatively more likely to experience erosion have higher values. (Derived from USGS Blackbird Mountain DEM, 10-m resolution, and IKONOS imagery, 4-m resolution).

DISCUSSION

FIELD STUDY

The relative hazard maps using field data incorporated the parameters of slope, aspect, burn severity, hydrology, geology, and soil characteristics for landslides; and slope, aspect, burn severity, understory vegetation cover, hydrology, geology, and soil characteristics for erosion.

Field mapping was performed at scales appropriate to the parameters being mapped. For example, burn severity was mapped at a scale of tens-of-meters, whereas hydrology was mapped at meter-scale resolution. The relative hazard maps of all three sites generated with field data correspond well to observations made in the field regarding areas relatively more likely to experience landslides and erosion. Areas of highest relative risk to landslides and erosion are assumed to be those within 40-50% of the maximum ranking values. Therefore, areas of highest relative risk to landslides have values of 25 and greater and areas of highest relative risk to erosion have values of 30 and greater.

Site #1: Quartzite Mountain
The areas of highest relative risk to landslides are those areas with slopes greater than 34º, surface water, and low to high burn severities. These areas are located in the northeast and southwest portions of the site. The areas of highest relative risk to erosion are those areas with north-facing slopes greater than 29º, moderate to high burn severities, 0-25% understory vegetation cover, and surface water. These areas are located in the southern and eastern portions of the site. These results agree with field observations because steep slopes, surface water, and low to high burn severities are all represented by high values in the ranking system. The geology and soil characteristics are consistent throughout the site, so they do not influence spatial changes in the hazard maps. During field study in July 2002, centimeter-scale rilling over an area approximately 5 m² was observed in the southwest corner of the site in the same area predicted by the hazard maps to be susceptible to both landslides and erosion.

Site #2: Fourth of July Creek
The areas of highest relative risk to landslides are those areas with slopes greater than 34º and low to high burn severities. These areas are located in the southern and northwest portions of the site. The areas of highest relative risk to erosion are those areas with north-facing slopes greater than 20º, moderate to high burn severities, and 0-25% understory vegetation cover. These areas are also located in the southern and northwest portions of the site. The presence of clayey-sandy silt (ranked with a value of 5) along the eastern portion of the site does not significantly influence the overall risk assessment. The geology is consistent throughout the site and there is no surface water, so these parameters do not influence spatial changes in the hazard maps.

Site #3: Lake Creek
The areas of highest relative risk to landslides are those areas with slopes greater than 34º, surface water, and low to high burn severities. These areas are located throughout the western and southern portions of the site. The areas of highest relative risk to erosion are those areas with north-facing slopes greater than 34º, low to high burn severities, and surface water. These areas are also located throughout the western and southern portions of the site. Geology and soil characteristics vary only slightly throughout the site, and do not influence spatial changes in the hazard maps. Surprisingly, understory vegetation cover does not appear to significantly influence the erosion hazard map. This may be because slope, burn severity, and surface water are more heavily weighted in the ranking system and thus override the effects of understory vegetation cover.

Summary
For Sites #1-3, the areas of highest relative risk to landslides are those areas with slopes greater than 34º, surface water (except Site #2, which has no surface water), and low to high burn severities. This is to be expected, as these three parameters are given the highest weighting in the overall ranking system.

The areas in Sites #1-3 of highest relative risk to erosion are the steepest, north-facing slopes. Sites #1 and #2 are influenced by moderate to high burn severities and low understory vegetation cover (0-25%). Site #3 exhibits more burn severity heterogeneity and so is influenced by a larger range of burn severities (low to high), and does not appear to be affected by understory vegetation cover. Sites #1 and #3 are affected by surface water, but again, Site #2 has no surface water.

REMOTE SENSING
The relative hazard maps using remote sensing data incorporated the parameters of slope, aspect, burn severity, and geology for landslides; and slope, aspect, burn severity, vegetation cover, and geology for erosion. In general, the relative hazard maps for each site generated with remote sensing data correspond well to areas predicted from field mapping. The greatest difference is that the remote sensing imagery classifies each 4-m pixel, whereas field mapping tends to group areas together at scales of tens-of-meters. Areas of highest relative risk to landslides and erosion are assumed to be those within 30-35% of the maximum ranking values. Therefore, areas of highest relative risk to landslides have values of 20 and greater and areas of highest relative risk to erosion have values of 22 and greater.

Most of the surface water within Sites #1 and #3 is in the form of small springs and streams less than 2 m, which cannot be detected by remote sensing data. This omission significantly affected the comparisons between field mapping and remote sensing data because areas with surface water present were assigned a high value (10) in the ranking system. Areas with surface water are significantly more likely to experience landslides and erosion than in areas without surface water. In order to detect the water bodies found in the study sites, remote sensing imagery with at least 1-m resolution would be required. A higher-resolution platform than IKONOS, such as Digital Globe's Quickbird (2.4 m multispectral resolution and 0.6 m panchromatic resolution), may provide such resolution; however, the cost of this data may be prohibitive for large areas such as the SCNF. Another consideration is that surface water fluctuates seasonally, and thus the season at which remote sensing imagery is acquired becomes more important. In addition, springs are often obscured by vegetation.

Soil is an important parameter because soils can influence landslides and erosion due to their infiltration capacities and the ease by which they may be transported. Unfortunately, it is difficult to evaluate soil type directly with IKONOS or similar multispectral remote sensing platforms. Although hyperspectral remote sensing platforms can be used to evaluate soil mineralogy, these platforms cannot be used to directly analyze grain size. In addition, heavily vegetated areas such as the study areas prevent direct observation of the ground.

It is important to note that the NDVI transformation used to assess vegetation cover cannot distinguish between understory and overstory vegetation cover. Remote sensing classifications

for burn severity and vegetation cover may overlap, causing the results to be overpredictive. Conversely, if the overstory is unburned and the understory is burned, results may be underpredictive. Another potential problem with using NDVI values is that this transformation does not model areas of exposed soil well. This is because soil may contain organic materials and chemical constituents that will influence the reflectivity from the red band.

Statistical Evaluation of Minimum Distance Classifications

The accuracy of the minimum distance classifications was assessed using the bootstrap method. A confusion matrix was generated to show the accuracy of each classification by comparing the classification results with ground-truth information (i.e. bootstrap training sites). The overall accuracy (total number of pixels classified correctly divided by the total number of pixels), kappa coefficient, confusion matrix, errors of commission (percentage of extra pixels in class), errors of omission (percentage of pixels left out of class), producer accuracy (probability that a pixel in the classification image is put into class *X* given the ground-truth class is *X)*, and user accuracy (probability that the ground-truth class is *X* given a pixel is put into class *X* in the classification image) was assessed for Sites #1-4 (Tables 8-11). For Site #1, the overall accuracy is 82.27% and K = 0.69. For Site #2, the overall accuracy is 62.40% and K = 0.50. For Site #3, the overall accuracy is 72.82% and K = 0.52. For Site #4, the overall accuracy is 71.04% and K = 0.59. Although these values are relatively high for remote sensing classifications, the errors of commission and omission are high in some cases. For example, in Site #1, low and high severity burns were often incorrectly classified as moderate severity burns, resulting in a high error of commission (81.61%). In Site #2, unburned and moderate severity burns were incorrectly classified as low severity burns, resulting in a commission error of 50.73%. Low severity burns were classified as unburned and moderate severity

Table 8. The overall accuracy, kappa coefficient, confusion matrix, errors of commission and omission, and producer and user accuracy assessed for the minimum distance classification of Site #1.

Minimum Distance Classification	Ground-Truth Pixels					
	High Reflectance	Unburned	Low Severity	Moderate Severity	High Severity	Total
Unclassified	0	0	0	0	0	0
High Reflectance	327	0	0	0	0	327
Unburned	0	106	157	14	0	277
Low Severity	0	22	502	21	0	545
Moderate Severity	34	3	206	98	192	533
High Severity	14	0	78	37	2578	2707
Total	375	131	943	170	2770	4389
Commission (%)	0.00	61.73	7.89	81.61	4.77	
Omission (%)	12.80	19.08	46.77	42.35	6.93	
Producer Accuracy (%)	87.20	80.92	53.23	57.65	93.07	
User Accuracy (%)	100.00	38.27	92.11	18.39	95.23	
Overall Accuracy 82.27%						
Kappa Coefficient = 0.69						

Table 9. The overall accuracy, kappa coefficient, confusion matrix, errors of commission and omission, and producer and user accuracy assessed for the minimum distance classification of Site #2.

Minimum Distance Classification	Ground-Truth Pixels					
	High Reflectance	Unburned	Low Severity	Moderate Severity	High Severity	Total
Unclassified	0	0	0	0	0	0
High Reflectance	332	0	8	0	0	340
Unburned	0	1598	155	879	0	2632
Low Severity	105	183	539	262	5	1094
Moderate Severity	2	873	276	1434	10	2595
High Severity	2	38	37	419	1497	1993
Total	441	2692	1015	2994	1512	8654
Commission (%)	2.35	39.29	50.73	44.74	24.89	
Omission (%)	24.72	40.64	46.90	52.10	0.99	
Producer Accuracy (%)	75.28	59.36	53.10	47.90	99.01	
User Accuracy (%)	97.65	60.71	49.27	55.26	75.11	
Overall Accuracy 62.40%						
Kappa Coefficient = 0.50						

burns, which resulted in an omission error of 52.10%. In Site #3, unburned and high severity burns were incorrectly classified as low severity burns, resulting in a commission error of 69.47%. Low severity burns were classified as unburned and high severity burns, which resulted in an omission error of 56.95%. Low and high severity burns were incorrectly classified as moderate severity burns, resulting in an error of commission of 56.81%. In Site #4, unburned and moderate severity burns were incorrectly classified as low severity burns, resulting in a commission error of 96.70%. Low severity burns were classified as unburned and high reflectance, which resulted in an omission error of 60.18%. Low and high severity burns were incorrectly classified as moderate severity burns, resulting in a commission error of 87.66%. Moderate severity burns were classified as unburned and high severity burns, which resulted in an omission error of 51.89%. This information indicates that areas of low and moderate burn severities particularly are not predicted well by the minimum distance classification for burn severity.

Taking into consideration the difficulties discussed above, the overall accuracies for Sites #1-4 are good (none less than 62.40%), and kappa values are all greater than 0.50. Site #1 yielded the highest overall accuracy and kappa values (82.27% and 0.69, respectively). This is probably because this site exhibits 80% high severity burns, which

Table 10. The overall accuracy, kappa coefficient, confusion matrix, errors of commission and omission, and producer and user accuracy assessed for the minimum distance classification of Site #3.

Minimum Distance Classification	Ground-Truth Pixels					
	High Reflectance	Unburned	Low Severity	Moderate Severity	High Severity	Total
Unclassified	0	0	0	0	0	0
High Reflectance	231	1	4	2	5	243
Unburned	0	795	118	24	26	963
Low Severity	0	239	229	68	214	750
Moderate Severity	21	1	41	450	529	1042
High Severity	0	23	140	174	2661	2998
Total	252	1059	532	718	3435	5996
Commission (%)	4.94	17.45	69.47	56.81	11.24	
Omission (%)	8.33	24.93	56.95	37.33	22.53	
Producer Accuracy (%)	91.67	75.07	43.05	62.67	77.47	
User Accuracy (%)	95.06	82.55	30.53	43.19	88.76	
Overall Accuracy 72.82%						
Kappa Coefficient = 0.52						

Table 11. The overall accuracy, kappa coefficient, confusion matrix, errors of commission and omission, and producer and user accuracy assessed for the minimum distance classification of Site #4.

Minimum Distance Classification	Ground-Truth Pixels					
	High Reflectance	Unburned	Low Severity	Moderate Severity	High Severity	Total
Unclassified	0	0	0	0	0	0
High Reflectance	7289	0	12	3	0	7304
Unburned	0	15957	145	2	0	16104
Low Severity	1110	5286	227	211	43	6877
Moderate Severity	9	2576	166	459	511	3721
High Severity	0	2854	20	279	8520	11673
Total	8408	26673	570	954	9074	45679
Commission (%)	0.21	0.91	96.70	87.66	27.01	
Omission (%)	13.31	40.18	60.18	51.89	6.11	
Producer Accuracy (%)	86.69	59.82	39.82	48.11	93.89	
User Accuracy (%)	99.79	99.09	3.30	12.34	72.99	
Overall Accuracy 71.04%						
Kappa Coefficient = 0.59						

are predicted well by the minimum distance classification. In general, it appears that the minimum distance classifications for burn severity correspond very well to the ground-truth or

validation areas mapped in the field. Sites #2, #3, and #4 had slightly lower overall accuracies (62.40%, 72.82%, and 71.04%, respectively) and kappa values (0.50, 0.52, and 0.59, respectively). These sites exhibit more burn heterogeneity, including more low and moderate severity burns, which were not predicted as well by the minimum distance classifications.

Site #1: Quartzite Mountain
With the remote sensing analysis, the areas of highest relative risk to landslides (values of 20 and greater) are those areas with slopes greater than 34º and moderate to high burn severities. These areas are located in the southwest portion of the site. The areas of highest relative risk to erosion (values of 22 and greater) are those areas with north-facing slopes greater than 19º, moderate to high burn severities, and 26-50% vegetative cover. These areas are located in the southern portion of the site. The geology is consistent throughout the site and thus does not influence spatial changes in the hazard maps. The minimum distance algorithm appears to correlate fairly well with burn severities observed in the field, although the western edge and northeastern portion of the site are classified as lower-severity burns than were observed in the field. The NDVI values appear to be more correlated to burn severity than to understory vegetation cover as mapped in the field. This site is dominated by high severity burns with little vegetation cover, so the large areas of bare soil present may affect the NDVI values as discussed above. In situations such as this, it may be advantageous to use SAVI rather than NDVI values. The rilling observed in the southwest corner of the site during field study in July 2002 is within the same area predicted by both the field-based and remotely-sensed hazard maps to be susceptible to both landslides and erosion.

Site #2: Fourth of July Creek
The areas of highest relative risk to landslides are those areas with slopes greater than 34º and low to high burn severities. These areas are located in the northeast and northwest portions and southern edge of the site. The areas of highest relative risk to erosion are those areas with north-facing slopes greater than 24º and low to high burn severities. These areas are located in the northeast and northwest portions and southern edge of the site. The geology is consistent throughout the site and thus does not influence spatial changes in the hazard maps. Vegetation cover does not appear to significantly influence the erosion hazard map results, which is likely due to the more heavily weighted parameters (slope, burn severity, and surface water) overriding the effects of vegetation cover. The minimum distance algorithm appears to correlate fairly well with high burn severity and unburned areas observed in the field except at the western edge of the site, where burn severity was underpredicted possibly due to areas of rock outcrop. Areas of low to moderate burn severity are also generally correlative with what was observed in the field. The NDVI values for this site appear to be better correlated to understory vegetation cover than to burn severity as mapped in the field. This is likely due to the fact that burn severity (and thus soil exposure) is more heterogeneous in this site.

Site #3: Lake Creek
The areas of highest relative risk to landslides are those areas with slopes greater than 34º and low to high burn severities. These areas occur throughout the site, except in the northwest corner where values are much lower. The areas of highest relative risk to erosion are those areas with north-facing slopes greater than 29º, low to high burn severities, and 26-75% vegetation cover. These areas also occur throughout the site, except in the northwest corner where values are much

lower. The geology varies but does not significantly influence overall hazard rankings. The minimum distance algorithm appears to correlate fairly well with burn severities observed in the field, although burn severity was underpredicted in the northeastern and southeastern portions of the site. The NDVI values for this site appear to be better correlated to understory vegetation cover than to burn severity as mapped in the field. Again, this may be due to the fact that burn severity (and thus soil exposure) is more heterogeneous in this site.

Site #4: Salmon-Challis National Forest
The highest relative values for both landslide and erosion hazards occur in the northwestern and southwestern portions of the site. These areas appear to be most influenced by slopes greater than 34° and moderate to high burn severities. This is expected, as these parameters are weighted most heavily in the ranking system. The parameters of aspect, geology, and vegetation vary throughout the site but do not significantly influence the overall hazard rankings because they were given less weight in the ranking system.

The burn intensities of Site #4 include all degrees of severity. For this particular site, training classes for the minimum distance algorithm were selected visually from the remote sensing data. Training classes were selected within Sites #1-3 for purposes of ground-truthing, and others were selected without the aid of field observations. It is important to collect training sites from areas distributed throughout the site so that influences of shadow and other variables in the imagery may be taken into account. Although training classes were selected from all slope aspects, it appears that many unburned areas in shadow were incorrectly classified as high severity burned areas. This may be corrected using several different methods including histogram stretching; topographic corrections based on sun elevation, sun azimuth angle, slope, and aspect; and masking shadowed areas by masking slopes with a particular slope angle and aspect .

Summary
For Sites #1-4, the areas of highest relative risk to landslides are those areas with slopes greater than 34º. Sites #2-4 exhibit more burn severity heterogeneity than Site #1 and thus they are influenced by a larger range of burn severities (low to high), whereas Site #1 is most affected by moderate to high burn severities. Steep slopes and low to moderate burn severities are given the highest weighting in the overall ranking system, so it is expected that these parameters would be most influential in the landslide hazard maps.

The areas in Sites #1-4 of highest relative risk to erosion are generally the steepest, north-facing slopes. Site #1 is influenced by moderate to high burn severities, whereas Sites #2 and #3 exhibit more burn severity heterogeneity and so are influenced by a larger range of burn severities (low to high). Site #1 is affected by moderate vegetation cover (26-50%), although the NDVI values appear to be more correlated to burn severity than to vegetation cover. This may be due to the large areas of bare soil present in this site. Site #3 is affected by a greater range of vegetation cover (26-75%). Sites #2 and #4 do not appear to be influenced by vegetation cover, which may be due to the more heavily weighted parameters (slope and burn severity) overriding the effects of vegetation cover.

STATISTICAL COMPARISON OF FIELD AND REMOTE SENSING DATA
Statistical comparisons between field mapping results and remote sensing data were obtained by calculating the kappa coefficient, K. This is a direct, pixel-by-pixel comparison, rather than a

comparison between groups of pixels as in the traditional bootstrap accuracy check. It was not necessary to compare slope and aspect between field mapping results and remote sensing data because they were assessed using the same data source (USGS 10-m DEMs). Burn severity, vegetation cover, and geology for each site were compared individually and the results discussed below. As previously stated, the range of K is 0-1, with zero corresponding to chance agreement and 1 corresponding to perfect agreement.

Site #1: Quartzite Mountain

The remote sensing data for burn severity was compared to field mapping results using a 4x4 confusion matrix (because there were four different ranking values for burn severity in this site) (Table 12). Although the remote sensing data visually appear to predict the areas of high burn severity well, the comparison yielded K = 0.15.

In order to ascertain whether the classification system for burn severity could be improved, the ranking values for burn severity were reclassified. The first reclassification grouped unburned and low severity burns together and assigned them a value of 2 (Table 13). Moderate and high burn severity were grouped together and assigned a value of 10. Recalculating kappa resulted in K = 0.39, which is a substantial improvement. A second reclassification maintained the original values for unburned and high burn severity (zero and 10, respectively) but grouped low and moderate severity burns and assigned these areas a value of 9 (Table 14). Recalculating kappa resulted in K = 0.15, which is the same as the original. A third reclassification grouped all areas into two classes, either unburned (assigned a value of zero) or burned (assigned a value of 10) (Table 15). This yielded K = 0.27, which is a notable improvement. Overall, it appears that the first reclassification yields the best results for this site (K = 0.39). This is most likely attributed to 80% of the total site area exhibiting high burn severity, which was predicted well by the remote sensing data.

Table 12. The 4x4 confusion matrix used to assess the accuracy of the remote sensing burn severity data to field mapping results at Site #1. Ranking values are noted in parentheses. Shaded areas contain actual number of pixels.

		Remote Sensing Reclassification Values			
		1 (0)	**5 (8)**	**11 (9)**	**19 (10)**
Field Mapping Reclassification Values	**25 (0)**	468	237	346	191
	50 (8)	650	1068	876	1823
	75 (9)	91	68	944	3176
	100 (10)	791	1696	8172	31,508
		K = 0.15			

Table 13. The 2x2 confusion matrix used to assess the accuracy of reclassified remote sensing burn severity data to field mapping results at Site #1. Ranking values are noted in parentheses. Shaded areas contain actual number of pixels.

		Remote Sensing Reclassification Values	
		1 (2)	**5 (10)**
Field Mapping Reclassification Values	**25 (2)**	2423	3236
	50 (10)	2646	43800
		K = 0.39	

Table 14. The 3x3 confusion matrix used to assess the accuracy of reclassified remote sensing burn severity data to field mapping results at Site #1. Ranking values are noted in parentheses. Shaded areas contain actual number of pixels.

		Remote Sensing Reclassification Values		
		1 (0)	**5 (9)**	**11 (10)**
Field Mapping Reclassification Values	**25 (0)**	468	583	191
	50 (9)	741	2956	4999
	75 (10)	791	9868	31,508
		K = 0.15		

Table 15. The 2x2 confusion matrix used to assess the accuracy of reclassified remote sensing burn severity data to field mapping results at Site #1. Ranking values are noted in parentheses. Shaded areas contain actual number of pixels.

		Remote Sensing Reclassification Values	
		1 (0)	**5 (10)**
Field Mapping Reclassification Values	**25 (0)**	468	774
	50 (10)	1532	49,331
		K = 0.27	

The remote sensing data for vegetation cover was compared to the field mapping results using a 2x2 confusion matrix. The field mapping results have rankings of 2 and 5, and the remote sensing results have rankings of 2, 3, and 4. Therefore, rankings were reclassified into values of 2 and not 2 (Table 16). This comparison yielded K = 0.16.

In order to evaluate whether the classification system for vegetation cover could be improved, the ranking values were reclassified (Table 17). A visual inspection of the remote sensing data for this site indicates that high burn severity areas have NDVI values less than -0.05 and

unburned areas have NDVI values greater than 0.2. Therefore, ranking values were reclassified so that NDVI values from -1 to 0.2 had a value of 5, and NDVI values from 0.2 to 1 had a value of 2. This resulted in K = 0.33, which is a substantial improvement and indicates difficulty in correctly predicting areas of intermediate vegetation cover.

The geology of the remote sensing data agreed perfectly with the field mapping results and because there were no discrepancies, K = 1.0.

Table 16. The 2x2 confusion matrix used to assess the accuracy of the remote sensing vegetation cover data to field mapping results at Site #1. Ranking values are noted in parentheses. Shaded areas contain actual number of pixels.

		Remote Sensing Reclassification Values	
		1 (2)	**5 (not 2)**
Field Mapping Reclassification Values	**25 (2)**	491	10,379
	50 (not 2)	158	45,246
		K = 0.16	

Table 17. The 2x2 confusion matrix used to assess the accuracy of the reclassified remote sensing vegetation cover data to field mapping results at Site #1. Ranking values are noted in parentheses. Shaded areas contain actual number of pixels.

		Remote Sensing Reclassification Values	
		1 (2)	**5 (5)**
Field Mapping Reclassification Values	**25 (2)**	4267	6603
	50 (5)	4187	41,217
		K = 0.33	

Site #2: Fourth of July Creek

The remote sensing data for burn severity was compared to the field mapping results using a 4x4 confusion matrix (because there were four different ranking values for burn severity in this site) (Table 18). This comparison yielded K = 0.22. The remote sensing data predicts areas of high burn severity very well.

The values for burn severity were reclassified the same as for Site #1. The first reclassification grouped unburned and low severity burns together and assigned them a value of 2 (Table 19). Moderate and high burn severity were grouped together and assigned a value of 10. Recalculating kappa resulted in K = 0.18, indicating this is not a better classification than the original. A second reclassification maintained the original values for unburned and high burn severity (zero and 10, respectively) but grouped low and moderate severity burns and assigned these areas a value of 9 (Table 20). Recalculating kappa resulted in K = 0.27, which is an

improvement. A third reclassification grouped all areas into two classes, either unburned (assigned a value of zero) or burned (assigned a value of 10) (Table 21). This yielded K = 0.28, which is similar to the second reclassification. Overall, it appears that the second and third reclassifications yield the best results for this site. This is probably because burn severity is highly variable within this site, and field mapping results indicate 29% of the total site area is unburned.

Table 18. The 4x4 confusion matrix used to assess the accuracy of the remote sensing burn severity data to field mapping results at Site #2. Ranking values are noted in parentheses. Shaded areas contain actual number of pixels.

		Remote Sensing Reclassification Values			
		1 (0)	**5 (8)**	**11 (9)**	**19 (10)**
Field Mapping Reclassification Values	**25 (0)**	7841	4981	6897	1254
	50 (8)	676	4468	2516	2174
	75 (9)	5085	7034	6780	3862
	100 (10)	246	3316	2963	9445
		K = 0.22			

Table 19. The 2x2 confusion matrix used to assess the accuracy of reclassified remote sensing burn severity data to field mapping results at Site #2. Ranking values are noted in parentheses. Shaded areas contain actual number of pixels.

		Remote Sensing Reclassification Values	
		1 (2)	**5 (10)**
Field Mapping Reclassification Values	**25 (2)**	17,966	12,841
	50 (10)	15,681	23,050
		K = 0.18	

Table 20. The 3x3 confusion matrix used to assess the accuracy of reclassified remote sensing burn severity data to field mapping results at Site #2. Ranking values are noted in parentheses. Shaded areas contain actual number of pixels.

		Remote Sensing Reclassification Values		
		1 (0)	**5 (9)**	**11 (10)**
Field Mapping Reclassification Values	**25 (0)**	7841	11,878	1254
	50 (9)	5761	20,798	6036
	75 (10)	246	6279	9445
		K = 0.27		

Table 21. The 2x2 confusion matrix used to assess the accuracy of reclassified remote sensing burn severity data to field mapping results at Site #2. Ranking values are noted in parentheses. Shaded areas contain actual number of pixels.

		Remote Sensing Reclassification Values	
		1 (0)	**5 (10)**
Field Mapping Reclassification Values	**25 (0)**	7841	13,132
	50 (10)	6007	42,558
		K = 0.28	

The remote sensing data for vegetation cover was compared to the field mapping results using a 3x3 confusion matrix. The field mapping results have rankings of 2, 4, and 5, and the remote sensing results have rankings of 2, 3, and 4. Therefore, rankings were reclassified into values of 2, 4, and not 2 or 4 (Table 22). This comparison yielded K = 0.01.

The ranking values for vegetation cover were then reclassified in the same manner as for Site #1 (Table 23). Visual inspection of the remote sensing data for this site indicates that high burn severity areas have NDVI values less than -0.05 and unburned areas have NDVI values greater than 0.2. Therefore, ranking values were reclassified so that NDVI values from -1 to 0.2 had a value of 5, and NDVI values from 0.2 to 1 had a value of 2. This resulted in K = 0.17, which is a substantial improvement.

The geology of the remote sensing data agreed perfectly with the field mapping results and because there were no discrepancies, K = 1.0.

Table 22. The 3x3 confusion matrix used to assess the accuracy of the remote sensing vegetation cover data to field mapping results at Site #2. Ranking values are noted in parentheses. Shaded areas contain actual number of pixels.

		Remote Sensing Reclassification Values		
		1 (2)	**5 (4)**	**11 (not 2 or 4)**
Field Mapping Reclassification Values	**25 (2)**	9540	1083	38,846
	50 (4)	3163	584	15,379
	75 (not 2 or 4)	18	688	2958
		K = 0.01		

Table 23. The 2x2 confusion matrix used to assess the accuracy of the reclassified remote sensing vegetation cover data to field mapping results at Site #2. Ranking values are noted in parentheses. Shaded areas contain actual number of pixels.

		Remote Sensing Reclassification Values	
		1 (2)	**5 (5)**
Field Mapping Reclassification Values	**25 (2)**	33,942	12,940
	50 (5)	11,856	9704
		K = 0.17	

Site #3: Lake Creek

The remote sensing data for burn severity was compared to the field mapping results using a 4x4 confusion matrix (because there were four different ranking values for burn severity in this site) (Table 24). This comparison yielded K = 0.16. The remote sensing data predicts areas of high burn severity well.

The values for burn severity were then reclassified the same as for Sites #1 and #2. The first reclassification grouped unburned and low severity burns together and assigned them a value of 2 (Table 25). Moderate and high burn severity were grouped together and assigned a value of 10. Recalculating kappa resulted in K = 0.27, which is a notable improvement. A second reclassification maintained the original values for unburned and high burn severity (2 and 10, respectively) but grouped low and moderate severity burns and assigned these areas a value of 9 (Table 26). Recalculating kappa resulted in K = 0.16, indicating this is not a better classification than the original. A third reclassification grouped all areas into two classes, either unburned (assigned a value of zero) or burned (assigned a value of 10) (Table 27). This yielded K = 0.32, which is a substantial improvement. Overall, it appears that the third reclassification yields the best results for this site. This is probably because burn severity is highly variable within this site, and field mapping results indicate 27% of the total site area is unburned.

The remote sensing data for vegetation cover was compared to the field mapping results using a 3x3 confusion matrix (both field mapping and remote sensing results have rankings of 2, 3, and 4) (Table 28). This comparison yielded K = 0.06.

Table 24. The 4x4 confusion matrix used to assess the accuracy of the remote sensing burn severity data to field mapping results at Site #3. Ranking values are noted in parentheses. Shaded areas contain actual number of pixels.

		Remote Sensing Reclassification Values			
		1 (0)	**5 (8)**	**11 (9)**	**19 (10)**
Field Mapping Reclassification Values	**25 (0)**	6048	4825	1070	2439
	50 (8)	215	504	439	1007
	75 (9)	1036	2268	3308	3713
	100 (10)	3685	7665	4855	11,035
		K = 0.16			

Table 25. The 2x2 confusion matrix used to assess the accuracy of reclassified remote sensing burn severity data to field mapping results at Site #3. Ranking values are noted in parentheses. Shaded areas contain actual number of pixels.

		Remote Sensing Reclassification Values	
		1 (2)	**5 (10)**
Field Mapping Reclassification Values	**25 (2)**	11,592	4955
	50 (10)	14,654	22,911
		K = 0.27	

Table 26. The 3x3 confusion matrix used to assess the accuracy of reclassified remote sensing burn severity data to field mapping results at Site #3. Ranking values are noted in parentheses. Shaded areas contain actual number of pixels.

		Remote Sensing Reclassification Values		
		1 (2)	**5 (9)**	**11 (10)**
Field Mapping Reclassification Values	**25 (2)**	6048	5895	2439
	50 (9)	1251	6519	4720
	75 (10)	3685	12,520	11,035
		K = 0.16		

Table 27. The 2x2 confusion matrix used to assess the accuracy of reclassified remote sensing burn severity data to field mapping results at Site #3. Ranking values are noted in parentheses. Shaded areas contain actual number of pixels.

		Remote Sensing Reclassification Values	
		1 (0)	**5 (10)**
Field Mapping Reclassification Values	**25 (0)**	6048	8334
	50 (10)	4936	34,794
		K = 0.32	

The ranking values for vegetation cover were then reclassified the same as was done for Sites #1 and #2 (Table 29). Visual inspection of the remote sensing data for this site indicates that high-severity burned areas have NDVI values less than -0.05 and unburned areas have NDVI values greater than 0.2. Ranking values were thus reclassified so that NDVI values from -1 to 0.2 had a value of 5, and NDVI values from 0.2 to 1 had a value of 2. This resulted in K = 0.14, which is a notable improvement.

Table 28. The 3x3 confusion matrix used to assess the accuracy of the remote sensing vegetation cover data to field mapping results at Site #3. Ranking values are noted in parentheses. Shaded areas contain actual number of pixels.

		Remote Sensing Reclassification Values		
		1 (2)	**5 (3)**	**11 (4)**
Field Mapping Reclassification Values	**25 (2)**	5951	30,851	482
	50 (3)	263	10,356	679
	75 (4)	309	7265	554
		K = 0.06		

Table 29. The 2x2 confusion matrix used to assess the accuracy of the reclassified remote sensing vegetation cover data to field mapping results at Site #3. Ranking values are noted in parentheses. Shaded areas contain actual number of pixels.

		Remote Sensing Reclassification Values	
		1 (2)	**5 (5)**
Field Mapping Reclassification Values	**25 (2)**	32,396	16,186
	50 (5)	3485	4643
		K = 0.14	

The remote sensing data for geology was compared to the field mapping data by using a 2x2 confusion matrix (because there were 2 different ranking values for geology in this site, 2 and 3) (Table 30). This resulted in K = 0.63.

Table 30. The 2x2 confusion matrix used to assess the accuracy of the remote sensing geology data to field mapping results at Site #3. Ranking values are noted in parentheses. Shaded areas contain actual number of pixels.

		Remote Sensing Reclassification Values	
		1 (2)	**5 (3)**
Field Mapping Reclassification Values	**25 (2)**	793,867	62,353
	50 (3)	12,117	78,532
		K = 0.63	

To summarize the findings for Sites #1-3, it appears that the first reclassification, which grouped unburned and low severity burns together and moderate and high burn severity together, yielded the highest kappa (0.39) for Site #1. This is probably because 80% of the total site area has high burn severity, which was predicted well by the remote sensing data. The third reclassification, which grouped all areas into classes of either unburned or burned, yielded the highest kappas for Sites #2 and #3 (0.28 and 0.32, respectively). This is attributed to the highly variable burn severity within these two sites. The minimum distance classifications do not predict areas of low and moderate severities as well as unburned and high severity burn areas.

In Sites #1-3, the kappa values for vegetation cover were low (0.16, 0.01, and 0.06, respectively). When the ranking values were reclassified so NDVI values from -1 to 0.2 had a value of 5 and NDVI values from 0.2 to 1 had a value of 2, the kappa values improved substantially (0.33, 0.17, and 0.14, respectively). It is not clear whether this is a true improvement, or is the result of reducing the number of classes compared (four for the original and two for the reclassification). There are two possible explanations for the low kappa values in vegetation cover. First, the NDVI transformations may not distinguish between understory and overstory vegetation cover. Second, NDVI values may be affected by high reflectivity soils.

The geology for Sites #1-3 was well predicted by the remote sensing data (i.e., the digitized compilation geology map). The geology of the remote sensing data agreed perfectly with the field mapping results in Sites #1 and #2, so K = 1.0. The remote sensing data for geology in Site #3 differed only slightly from the field mapping data, such that K = 0.63.

CLIMATE CONSIDERATIONS

Drought conditions, which have affected the study areas, have made it impossible to test the predictions made by the relative hazard maps. As noted by National Climatic Data Center

(2003), the current national-scale drought began in November 1999 and first peaked in August 2000. The drought peaked again in July 2002. Therefore, there simply has not been enough water (i.e. snow pack) available to initiate landslides or erosion since the wildfires of 2000.

CONCLUSIONS

This study demonstrates that remote sensing imagery is a promising tool in predicting areas of potential landslide and soil erosion hazards as a result of wildfire activity. For this study, remote sensing and DEM analyses can be used to evaluate slope, aspect, burn severity, and vegetation cover, which are important factors in determining landslide and erosion hazards. However, these analyses cannot be used to evaluate hydrology, geology, and soil characteristics. The methodology developed in this study is applicable for identifying and mapping landslide and erosion hazards in large, remote areas that have limited access. This is especially significant for land management, because this methodology requires fewer personnel and takes less time than traditional field mapping techniques. It is therefore a less expensive undertaking, even considering the cost of high-resolution remote sensing data. Another valuable aspect of this methodology is that it can be performed much quicker than field mapping, thus enabling land managers to respond faster and more efficiently with landslide and erosion mitigation efforts.

The types of remote sensing data most useful in this methodology are IKONOS data and USGS 10-m DEM's. IKONOS is fairly expensive, and thus the methodology developed for this study may also be performed using Landsat data for a significant cost reduction. If Landsat data are to be used, it would be most practical to use USGS 30-m DEM's because the compilation risk maps will only be as accurate as the coarsest-resolution source data available. In addition, USGS 30-m DEM's are more widely available than 10-m DEM's. An important consideration is the ability to obtain remote sensing imagery with resolutions sufficient for mapping site-specific parameters. The resolution of the remote sensing data should be appropriate for the particular hillslope processes being assessed.

It is important to note that relative hazard classification systems should be developed specifically for the regional area to be assessed. Classification systems may consider site-specific parameters, but should certainly include parameters of slope, burn severity, surface hydrology, understory vegetation cover (for erosion only), and soil characteristics. These parameters are all weighted most heavily in this study. Although understory vegetation cover and soil characteristics are generally considered to be significant factors influencing hillslope processes, field observations in Sites #1-3 do not indicate that these parameters substantially influence the likelihood of landslides and erosion. The parameters of aspect, geology, and are also important, but may not contribute significantly to the overall hazard maps and were ranked accordingly for this study. Obviously, the more parameters are used for assessment, the more comprehensive the hazard maps will be.

Either a supervised classification or NDVI transformation may be used to assess burn severity, although this study found a supervised classification to be most correlative to field mapping results. If both types of algorithms are used (as with this study), it should be noted that NDVI transformations cannot distinguish between understory and overstory vegetation cover. For example, a high NDVI value may be obtained from an area with burned understory and unburned overstory. This would be underpredictive and result in a low hazard ranking. In addition, results

for burn severity and vegetation cover assessment may overlap, causing the findings to be overpredictive. Another potential problem with using NDVI values is that this transformation is affected by high reflectivity soils. In areas with high soil visibility, it may be more effective to use the SAVI or other vegetation indices that take soil into account.

Two methods were used to assess the accuracy of the remote sensing classifications. The bootstrap method, which compares field-validated data to remote sensing classifications, yielded kappa values equal to or greater than 0.50. The second method was a direct, pixel-by-pixel comparison between field mapping and remote sensing classifications. The kappas produced with this method were equal to or less than 0.22. Visual comparisons between field mapping results and remote sensing data correlate fairly well; however, these kappa values yielded poorer results than expected.

There are several hypotheses for the differences in these kappa values. First, there may be slight differences between the georeferencing of the field and remote sensing data, which may be exaggerated by the pixel-by-pixel comparison. Second is the subjective bias at which boundaries are mapped in the field. Boundary locations and scale are subjective. This bias is not present in the 4-m resolution supervised classifications of the remote sensing data. Third, the remote sensing imagery classifies each 4-m pixel, whereas field mapping tends to group areas together at scales of tens-of-meters.

It is important to realize that kappa does not provide a measure of spatial correlation between two data sets. However, there may be an inherent difference in the spatial autocorrelation between the bootstrap and pixel-by-pixel methods. For example, the classes in the remote sensing data change more rapidly than the classes of the field mapping over a discrete spatial distance due to the remote sensing data 4-m pixel size. This spatial dependency is exaggerated in the pixel-by-pixel method (versus the bootstrap method). In other words, in the field mapping results, there is a higher likelihood that the pixel value at one geographic location will be related to the pixel next to it than in the pixel-by-pixel correlation.

The accuracies of the remote sensing burn severity classifications are dependent on the burn variability within the site. For example, Sites #2 and #3 yield the highest kappa values when burn severities are grouped into unburned and burned classes (K= 0.28 and K = 0.32, respectively). This is because these sites display a high degree of burn variability, and remote sensing classifications do not predict areas of low and moderate burn severity well. The highest kappa value for Site #1 is obtained by reclassifying the data into two classes, unburned to low burn severity, and moderate to high burn severity (K = 0.39). This is because Site #1 displays a low degree of burn variability and consists mostly of areas with high burn severity (80%). The most accurate comparisons for vegetation cover in Sites #1-3 occurred when NDVI values were reclassified into two classes. These classes include NDVI values from -1 to 0.2 and NDVI values from 0.2 to 1, and resulted in kappas of 0.33, 0.17, and 0.14 for Sites #1-3, respectively). It is not clear if this is a true improvement or is the result of reducing the number of classes (four for the original and two for the reclassification). Comparisons of geology were very accurate in Sites #1-3 (K = 1.0, K = 1.0, and K = 0.63, respectively); however, the compiled geologic map was based upon 1:100,00-scale field mapping performed by other geologists and was compared

to 1:24,000-scale field mapping done for this study, so this high degree of accuracy was expected.

Ground-truthing to assess the accuracy of the hazard maps created for Site #4 is beyond the scope of this study. Because this site was only validated against Sites #1-3, it should be ground-truthed more rigorously prior to being used by land managers in the SCNF. In order to perform ground-truthing, a validation strategy must be developed for selecting ground-truthing locations. This may be performed with grid or random point sampling. The ground-truth data will provide information regarding commission and omission errors, which may be used to evaluate the degree to which parameters included in the hazard maps are predicted correctly and incorrectly. Ground-truth data should also be assessed for which parameters contribute most significantly to landslide and erosion hazards in order to evaluate the ranking systems developed in this study.

ACKNOWLEDGEMENTS
I am grateful to Nancy Glenn, Glenn Thackray, and Paul Link for their expertise and guidance over the past three years. I thank the following people for their support and advice: Keith Weber, Linda Davis, John Welhan, Melissa Merrick, Chris Moller, Betsy Rieffenberger, and Jim Wolper. I feel lucky to have been part of the Geosciences Department Family – every member is supportive and encouraging, and their enthusiasm is contagious. This study was made possible by a fellowship from the NASA Sponsored Idaho Space Grant Consortium and grants from the Graduate Student Research and Scholarship Committee and the NASA Goddard Space Flight Center (ISU would like to acknowledge the Idaho Delegation for their assistance in obtaining this grant).

I thank my family for their love, patience, and unfailing support: Butch Wheeler, Mikki and Larrie Fitch, Del Sprague, Brian Sprague, Maxine and Don Foote, and Melanie and Alan Monson. Every good thing in my life is made possible by you. I am grateful to my best friends, who keep me grounded and in good spirits: Marcia Williams, Karen Edwards, Barbara Kracher, Duane DeVecchio, Tauna Butler, and Kebbie Wheeler. And to Butch Wheeler - the best husband, friend, and field assistant ever - it is difficult to articulate my love and gratitude. You make my world beautiful.

"It is never too late to be what you might have been." – George Eliot

LITERATURE CITED

Bailey, R.G., 1971, Landslide Hazards Related to Land Use Planning in Teton National Forest, Northwest Wyoming: U.S. Department of Agriculture Report, 131 p.

Benavides-Solorio, J., and MacDonald, L.H., 2001, Post-fire runoff and erosion from simulated rainfall on small plots, Colorado Front Range: Hydrological Processes, v. 15, p. 2931-2952.

Cannon, S.H., 2001, Debris-flow generation from recently burned watersheds: Environmental and Engineering Geoscience, v. 7, no. 4, p. 321-341.

Cannon, S.H., Bigio, E.R., Mine, E., 2001a, A process for fire-related debris flow initiation, Cerro Grande fire, New Mexico: Hydrological Processes, v. 15, p. 3011-3023.

Cannon, S.H., Kirkham, R.M., and Parise, M., 2001b, Wildfire-related debris-flow initiation processes, Storm King Mountain, Colorado: Geomorphology, v. 39, p. 171-188.

Carey, A., and Carey, S., 1989, Yellowstone's Red Summer: Flagstaff, AZ, Northland Publishing, 114 p.

Churchill, R.R., 1982, Aspect-induced differences in hillslope processes: Earth Surface Processes and Landforms, 7: 171-182.

Clayton, J.L., and Megahan, W.F., 1986, Erosional and chemical denudation rates in the southwestern Idaho batholith: Earth Surface Processes and Landforms, v. 11, p. 389-400.

Congalton, R.G., and Green, K., 1999, Assessing the Accuracy of Remotely Sensed Data: Principles and Practices: Boca Raton, FL, CRC Press, 137 p.

Cooke, R.U., and Doornkamp, J.C., 1990, Geomorphology in Environmental Management (2nd ed.): New York, NY, Oxford University Press, 410 p.

Crozier, M.J., Eyles, R.J., Marx, S.L., McConchie, J.A., and Owen, R.C., 1980, Distribution of landslips in the Wairarapa hill country: New Zealand Journal of Geology and Geophysics, v. 23, p. 575-586.

Doerr, S.H., Shakesby, R.A., and Walsh, R.P.D., 2000, Soil water repellency: its causes, characteristics, and hydro-geomorphological significance: Earth-Science Reviews, v. 51, no. 1-4, p. 33-65.

Dragovich, J.D., Brunengo, M.J., and Gerstel, W.J., 1993a, Landslide Inventory and Analysis of the Tilton River – Mineral Creek Area, Lewis County, Washington, Part 1: Terrain and Geological Factors: Washington Geology, v. 21, no. 3, p. 9-18.

Dragovich, J.D., Brunengo, M.J., and Gerstel, W.J., 1993b, Landslide Inventory and Analysis of the Tilton River – Mineral Creek Area, Lewis County, Washington, Part 2: Soils, Harvest Age, and Conclusions: Washington Geology, v. 21, no. 4, p. 18-30.

Dunne, T., and Leopold, L.B., 1978, Water in Environmental Planning: New York, NY, W.H. Freeman and Company, 818 p.

Easterbrook, D.J., 1999, Surface Processes and Landforms (2nd ed.): Saddle River, NJ, Prentice Hall, 546 p.

Ekren, E.B., 1988, Stratigraphic and structural relations of the Hoodoo Quartzite and Yellowjacket formation of Middle Proterozoic age from Hoodoo Creek eastward to Mount Taylor, central Idaho: U.S. Geological Survey Bulletin 1570, p. 1-17.

Environmental Systems Research Institute Inc., 2002, ArcView 3.3 and 8.2 Geographic Information System Software, Redlands, CA.

Evans, K.V., 1999, The Yellowjacket Formation of east-central Idaho, *in* Berg, R.B., ed., Belt Symposium III: Montana Bureau of Mines and Geology Special Publication 112, p. 17-30.

Evans, K.V., and Connor, J.J., 1993, Geologic map of the Blackbird Mountain 15-minute quadrangle, Lemhi County, Idaho: U.S. Geological Survey Miscellaneous Field Studies Map MF-2234, scale 1:62,500.

Fisher, F.S., and Johnson, K.M., 1995, Challis Volcanic Terrane, *in* Fisher, F.S., and Johnson, K.M., eds., Geology and Mineral Resource Assessment of the Challis 1° X 2° Quadrangle, Idaho: U.S. Geological Survey Professional Paper 1525, p. 41-43.

Gough, R.E., and Lamb, J., 2000, Fire-Resistant Plants for Montana Landscapes, available URL: http://www.montana.edu/wwwpb/pubs/mt200101.html, accessed April 13, 2003.

Gray, D.H., and Megahan, W.F., 1981, Forest vegetation and removal and slope stability in the Idaho batholith: USDA Forest Service Research Paper INT-271, 23 p.

Gritzner, M., Marcus, W.A., Aspinall, R., and Custer, S.G., 2000, Assessing landslide potential using GIS, soil wetness modeling and topographic attributes, Payette River, Idaho: Geomorphology, v. 37, p. 149-165.

Huete, A.R., 1988, A soil-adjusted vegetation index (SAVI): Remote Sensing of the Environment, v. 25, p. 295-309.

Huffman, E.L., MacDonald, L.H., and Stednick, J.D., 2001, Strength and persistence of fire-induced soil hydrophobicity under ponderosa and lodgepole pine, Colorado Front Range: Hydrological Processes, v. 15, p. 2877-2892.

Idaho Forest Products Commission, 2003, available URL: http://www.idahoforests.org/trees1.htm, accessed April 13, 2003.

Idaho Transportation Department, 1996, 1:100,000-Scale Metric Topographic Map of Challis, Idaho: scale 1:100,000.

Jensen, John R., 1996, Introductory Digital Image Processing (2nd ed.): Saddle River, NJ, Prentice Hall, 318 p.

Johansen, M.P., Hakonson, T.E., and Breshears, D.D., 2001, Post-fire runoff and erosion from rainfall simulation: contrasting forests with shrublands and grasslands: Hydrological Processes, v. 15, p. 2953-2965.

Keep Idaho Green, 2003, available URL: http://www.keepidahogreen.org/resident.htm,

accessed April 13, 2003.

Key, C.H., and Benson, N., 1999a, The Composite Burn Index (CBI): Field rating of burn severity, available URL: http://nrmsc.usgs.gov/research/cbi.htm, accessed September 30, 2002.

Key, C.H., and Benson, N., 1999b, The Normalized Burn Ration (NBR): A Landsat TM radiometric measure of burn severity, available URL: http://nrmsc.usgs.gov/research/ndbr.htm, accessed September 30, 2002.

Key, C.H., and Benson, N., 2002, Landscape Assessment, *in* Fire effects monitoring and inventory protocol, available URL: http://www.fire.org/firemon/lc.htm, accessed September 30, 2002.

Kimura, H., and Yamaguchi, Y., 2000, Detection of landslide areas using satellite radar interferometry: Photogrammetric Engineering and Remote Sensing, v. 66, no. 3, p. 337-344.

Kraemer, H.C., 1983, Kappa Coefficient: *in* Kotz, S. and N.L. Johnson, eds, Encyclopedia of Statistical Sciences: New York, NY, John Wiley and Sons, p. 352-354.

Koch, G.G., 1983, Hierarchical Kappa Statistics: *in* Kotz, S. and N.L. Johnson, eds, Encyclopedia of Statistical Sciences: New York, NY, John Wiley and Sons, p. 630-631.

Martin, D.A., and Moody, J.A., 2001, Comparison of soil infiltration rates in burned and unburned mountainous watersheds: Hydrological Processes, v. 15, p. 2893-2903.

McCarthy, D.F., 2002, Essentials of Soil Mechanics and Foundations (6th ed.): Saddle River, NJ, Prentice Hall, 788 p.

McKean, J., Buechel, S., and Gaydos, L., 1991, Remote Sensing and Landslide Hazard Assessment: Photogrammetric Engineering and Remote Sensing, v. 57, no. 9, p. 1185-1193.

Meyer, G.A., Pierce, J.L., Wood, S.H., and Jull, A.J.T., 2001, Fire, storms, and erosional events in the Idaho batholith: Hydrological Processes, v. 15, p. 3025-3038.

Meyer, G.A., Wells, S.G., Balling, R.C., Jr., and A.J.T. Jull, 1992, Response of alluvial systems to fire and climate change in Yellowstone National Park: Letters To Nature, v. 357, p. 147-150.

Moeremans, B., and Dautrebande, S., 2000, Soil moisture evaluation by means of multitemporal ERS SAR PRI images and interferometric coherence: Journal of Hydrology, v. 234, no. 3-4, p 162-169.

Nachtergaele, J., and Poesen, J., 1999, Assessment of soil losses by ephemeral gully erosion using high-altitude (stereo) aerial photographs: Earth Surface Processes and Landforms, v. 24, p. 693-706.

National Climatic Data Center, 2003, available URL: http://www.ncdc.noaa.gov/oa/climate/research/2003/feb/drought-national-overview.html#histfiles, accessed April 13, 2003.

National Interagency Fire Center (NIFC), 2001, available URL: http://www.nifc.gov, accessed October 16, 2002.

Pickup, G., and Marks, A., 2000, Identifying large-scale erosion and deposition processes from airborne gamma radiometrics and digital elevation models in a weathered landscape: Earth Surface Processes and Landforms, v. 25, p. 535-557.

Research Systems Inc., 2002, Environment for Visualizing Images (ENVI) Software, Boulder, CO.

Rieffenberger, B., 2000, USDA Forest Service Clear Creek Fire BAER Team Hydrology Report, Salmon-Challis National Forest, 21 p.

Ritter, D.F., Kochel, R.C., and Miller, J.R., 1995, Process Geomorphology (3rd ed.): Dubuque, IA, Wm. C. Brown Publishers, 546.

Ross, C.P., 1934, Geology and ore deposits of the Casto quadrangle, Idaho: U.S. Geological Survey Bulletin 854, p. 1-135.

Selby, M.J., 1993, Hillslope Materials and Processes (2nd ed.): New York, NY, Oxford University Press, 451 p.

Singhroy, V.H., Loehr, J.E., and Correa, A.C., 2000, Landslide risk assessment with high spatial resolution remote sensing satellite data: International Geoscience and Remote Sensing Symposium, Honolulu, 2000, Proceedings (URL: http://www.ccrs.nrcan.gc.ca/ccrs/rd/sci_pub/bibpdf/13012.pdf, accessed February 18, 2002).

Singhroy, V., and Mattar, K., 2000, SAR image techniques for mapping areas of landslides: International Society for Photogrammetry and Remote Sensing Conference, Amsterdam, 2000, Proceedings, p. 1395-1402.

Sohn, Y., and Rebello, N.S., 2002, Supervised and unsupervised spectral angle classifiers: Photogrammetric Engineering and Remote Sensing, v. 68, no. 12, p. 1271-1280.

Space Imaging, 2002, available URL: http://www.spaceimaging.com, accessed February 21, 2003.

Tysdal, R.G., 2000, Revision of Middle Proterozoic Yellowjacket Formation, Central Idaho: U.S. Geological Survey Professional Paper 1601-A, p. A1-A13.

United States Forest Service (USFS), 2001a, available URL: http://www.fs.fed.us/r4/sc, accessed October 16, 2002.

United States Forest Service (USFS), 2001b, A Report to the President in Response to the Wildfires of 2000, *in* National Fire Plan, available URL: http://www.fireplan.gov/president.cfm, accessed October 16, 2002.

Welhan, J., 2003, Geostatistics and Spatial Modeling: Idaho State University Department of Geosciences, Lecture Notes, p. 27-36.

Wilson, C.J., Carey, J.W., Beeson, P.C., Gard, M.O., and Lane, L.J., 2001, A GIS-based hillslope erosion and sediment delivery model and its application in the Cerro Grande burn area: Hydrological Processes, v. 15, p. 2995-3010.

Winston, Don, Link, P.K., and Hathaway, Nate, 1999, The Yellowjacket is not the Prichard and other heresies: Belt Supergroup Correlations, Structure and Paleogeography, east-central Idaho: *in* Hughes, S.S. and G.D. Thackray, eds, Guidebook to the Geology of Eastern Idaho: Pocatello, Idaho Museum of Natural History, p. 3-20.